ISOLDE Newsletter 2016

ISOLDE Workshop and Users Meeting 2015

In this issue

isolde.web.cern.ch

Introduction

M.J.G. Borge
ISOLDE leader & spokesperson

Different milestones were achieved during 2015. They have kept the community in continous excitement. A successful project should be based on a vibrant facility and that is what ISOLDE has proven to be over the last year. The year started very well with the technical team working hard to start the delivery of low energy beams in April. In parallel with great excitement we could witness how the extension hall was hosting new devices. The most noticeable and at the same time an important milestone was the arrival of the first superconducting cryomodule on the 2nd of May. An exponential increase of activity in the extension hall after that allowed the start of physics with post-accelerated beams in October. More details can be found in the different contributions in this newsletter.

The very first experiment carried out in April gave beautiful results and this success continued throughout the whole of 2015 in spite of the amount of technical issues that occurred mainly concentrated around the summer period. Thanks to the fast reaction of the technical groups the physics outcome was perserved. I would like to take the opportunity to thank them for that.

In total 33 experiments were realised and three letters of intent. This includes the time dedicated to the test of the new target for production of Boron, the three weeks dedicated to the production of negative ions and the three weeks dedicated to post-accelerate ^{74,76}Zn beams at 4MeV/u from the 22nd of October. This is a good balance between R&D and physics outcome.

It is certainly in our interest to push for beam developments and we do so in our periodic meetings of the Group of the Upgrade of ISOLDE (GUI). This group has as part of its mandate to identify programme-driven priorities for beam developments. In this respect the release of very difficult Boron beams was in the list with five LoI supporting its importance. The mandate of the GUI group goes beyond beam developments to all aspects of the Facility as can be read in: http://isolde.web.cern.ch/gui-mandate#overlay-context=group-upgrade-isolde-gui. Among them a new robust and reliable tape station to replace the existing one has been a priority of this group. The new tape station is ready and it will be placed at the hall in beam line LA2 during the 2016 beam time campaign to check its reliability and compare the results with the existing one. The present tape station will definitively be removed in the winter shutdown after more than 40 years of operation.

The building 508 was finished at the end of 2014, so the winter shut down was used to make operative the RILIS control room, the DAQ room and the Visitors room. It was impressive to see how extensibly these rooms were already used in 2015. In particular presentations for visitors were very soon given in building 508 with the advantage of the two panoramic windows looking into the hall. In fact in 2015 we had a record of 857 visitors and 65% of them received a presentation of the Facility in the visitor room of building 508. The furniture for the visitors room, the ISOLDE control room and the kitchen arrived in the second half of the year. Together with the different infrastructure put in place throughout the year we can consider that now building 508 is finished and constitutes a great improvement as working space in comparison with the previous complex of buildings (115, 507 and 601).

The complementarity between different devices and their state of the art capabilities allows pushing the limits of physics. This is one of the strong points of ISOLDE that facilitates its continuous success. This year the determination of the mean square radii of the n-deficient Hg and Au isotopes has been determined by pushing the sensitivity limits by combining state of the art techniques for production, separation and detection. Many other notable experiments took place during 2015 and the results are presented in individual contributions in this newsletter. We hope you enjoy the new newletter format coutesy of V. Manea.

Many of you will be travelling to ISOLDE for experiments in the coming months. It is a great pleasure to announce that EU Project, ENSAR2, grant agreement number 654002, submitted in September 2014 was approved in September last year and it started the 1st of March 2016. During this new project we expect to distribute transnational access funds equivalent to about two thousand two hundred days among young researchers,

students and new comers. This time the transnational access can be extended to our non-European partners.

The annual ISOLDE workshop and users meeting was held the 2-4 of December 2015 with more than 130 participants. The meeting benefited from an excellent choice of invited speakers, the remarkable quality of the presentations (http://indico.cern.ch/event/437713/) mainly by young researchers and the lively discussions and friendly atmosphere encountered during the poster session, the coffee breaks and the dinner at the Bois Joly in Crozet, France. The CERN DG, R. Heuer, closed the conference by presenting the four prizes sponsored by CAEN to the best posters and best young speakers, a consolidated tradition added to our annual ISOLDE meeting. R. Heuer also had the opportunity to play with the miniature Lego robot for ISOLDE. An outreach initiative of the University of Manchester to introduce 14-16 year old UK students to nuclear physics and by designing, the robot with LEGO pieces, to understand the difficulty of remote handling of radioactive material.

In the longer term, ISOLDE has been chosen to host the next edition of the International conference on Electromagnetic Isotope Separator and Related topics, EMIS2018. This will be a joint venture between the ISOLDE physics and technical group.

Many changes took place at the level of management, with the new CERN Director General Fabiola Gianotti taking the position in January 2016. Closer to us and very relevant was the change of Physics coordinator that happened on October 1st 2015. A special thank you should go to Magdalena Kowalska, whose work was instrumental in maintaining the Physics output at a good rate and whose help on many fronts was highly appreciated by all of us. Magda continues with us doing her own research in ultra-sensitive nuclear magnetic resonance, beta-NMR, in liquids for biophysics applications within her ERC grant. She already has a group and I foresee for her a bright future. She was replaced by Karl Johnston, so the coordinator position continues to be in good hands. The good knowledge of the facility and good communication between the previous and the new coordinators have made the change unnoticeable. This was crucial in the middle of the experimental campaign and within the start-up of HIE-ISOLDE.

As you may know we have a group meeting every Wednesday at 14:00 in the visitors room (26-1-022). When you have an experiment you are all welcome to attend the meeting or at least send a representative of the experiment to get the latest news and to inform us of the physics case to be studied. The meeting is followed by a seminar and you are very welcome and encouraged to present us your research. Please contact Stephan Malbrunot and/or me for fixing the date. I would like to take the opportunity to congratulate Stephan for his start ERC grant approved in December 2015. He will develop at ISOLDE within the frame of this ERC grant an ultra-sensitive system combining lasers with MR-ToF. I believe ISOLDE is the only experiment at CERN hosting two ERC winners. Their developments will enrich our program.

Already in the autumn, the preparation of the new long range plan was launched by the Nuclear Physics European Collaboration Committee, NuPECC. A large part of our community is involved in preparing the different chapters. The first draft will be ready for distribution before Christmas and the final discussion about the priorities concerning the different facilities in Europe will take place in Darmstadt 11-13 of January 2017.

Just before I finish I would like to take the opportunity to thank the technical and physicist teams that have made 2015 a successful year as witnessed by the contributions included below in this edition of the ISOLDE Newsletter. In 2016 HIE-ISOLDE will have two cryomodules finishing stage 1 of the project. A celebration for the stakeholders involved is planned for the 28th of September in the afternoon. We have again a very challenging year in front of us!

Information for users coming to ISOLDE 2016

Karl Johnston
ISOLDE physics coordinator

Changes to user registration for 2016

A full description of the procedure for registering at CERN is given below. Visiting teams should use the pre-registration tool (PRT) to register new users.

One important change for 2016: the teamleader and deputy teamleader who sends the information via PRT must have a valid CERN registration. This also applies to paper forms which have been signed at the visiting institute. If the teamleader or deputy do not have a valid registration, the Users office will refuse to accept the documents.

Safety at ISOLDE

Safety remains a priority at ISOLDE. As last year, there is a variety of safety courses both online (called SIR) and hands-on (CTA) which need to be followed by all users to gain access to ISOLDE. These are more precisely detailed in the section “How to obtain access to the ISOLDE hall”.

Contrary to 2015, there is now only one access required to enter ISOLDE, called ISOHALL. ISOWORK – which was in place during the civil engineering work for HIE-ISOLDE – has been suppressed. Physicists and users should enter ISOLDE through the tourniquet and door on the Jura side of ISOLDE, although those bringing equipment or cryogenics into the hall, can use the entrance at the SAS on the HIE-ISOLDE side. Access to ISOLDE is now exclusively via the dosimeter.

Newly enforced this year is the requirement to wear safety shoes and helmets within the ISOLDE hall. Spare helmets are available at the entrance. It is also mandatory to check yourself on the hand-foot monitor before leaving the ISOHALL zone. Hand foot monitors are available at both Jura and HIE-ISOLDE entrances; please use them.

Once within the ISOLDE hall you have at your disposal additional protective equipment such as gloves and contamination monitors to ensure your safety. These are located in the cupboard close to the old control room.

A variety of “expert” courses are available for those required to perform more demanding operations such as those involving cryogenics, using the crane and lasers. Please ensure that you have followed these courses before performing these tasks.

For those performing electrical work (e.g. making cables, putting up HV cages) – a 3-day CERN course needs to be followed (all local physicists have followed it). If you require more information about this, please do not hesitate to contact me.

The mechanical workshop in building 508 is fully operational. If you wish to use it a document will need to be provided which is signed by your teamleader, yourself, and our workshop supervisor, authorising you to use the selected machines in the workshop. For more information, please contact your experiment spokesperson or me.

The list of contacts for safety both for local experiments and visiting setups can be found here: http://isolde.web.cern.ch/safety. All visiting setups should ensure that they have had a safety inspection before their experiment starts at ISOLDE. Please allow sufficient time for this to be done. You can contact me for more information to prepare for this.

Removal and shipping of equipment from the ISOLDE hall

All equipment which has been in the ISOLDE experimental hall requires a control by radiation protection before it can be transported elsewhere or back to home institutes. A new “buffer zone” has been installed in the ISOLDE hall (close to the SAS and the HIE-ISOLDE tunnel) which implements the CERN-wide TREC system to ensure that all controlled equipment has traceability. This is now incorporated into the EDH flow for all transport requests from the ISOLDE hall.

Building 508: new control room

2016 sees the inauguration of the new control room in building 508. This allows users to set up and control their experiment in considerably more comfort than before. The new control room is located on the first floor of building 508 and is outside of the controlled area. Controls for beam gates and proton requests are also installed although the timing for the control of the beam gate remains in the old

control room. Two consoles will also remain in the old control room for local manipulations.

Building 508 and 275: labs, DAQ rooms and kitchen

On the ground floor of b508, within the CERN RP controlled area, the detector laboratory is now up and running, including recently-installed water cooling. The chemical laboratory is available for occasional chemical operations.

Upstairs in building 508 the kitchen is now fully installed comprising a fridge, cooker, microwave and dishwasher. In addition, a variety of coffee machines ranging from capsules to moka pots are available. Needless to say, this should be maintained in a good condition and it will be responsibility of experimental spokespeople to ensure that it is kept in a good state.

Users can also avail of the DAQ room to monitor their experiments outside of the controlled zone.

Building 275 has received a lot of attention in the past year. A complete refurbishment of the roof has taken place and the building is now being de-classified. At the time of writing, four rooms remain; the rest of the building including the old solid state laboratory and the central area are now considered de-classified. The former solid state laboratory will be available for installation and testing of equipment prior to installation in the ISOLDE hall. If you are interested in availing of this, please write to me with a detailed request of the infrastructural needs and the time expected.

Please contact me if you have questions concerning access and use of these labs.

The local physics team can also help you with many aspects of ISOLDE experiments, e.g. turbo and pre pumps, RP sources, chemicals, etc.

Visits to ISOLDE

Visits to ISOLDE are still possible. A typical visit consists of an overview presentation in the visitors' area in building 508 and – when possible – a tour of the ISOLDE facility itself along the pre-arranged visit path. In the event of a machine intervention or a conflict with physics which happens to be running, the tour of ISOLDE may be cancelled, and one remains in the 508 gallery area.

All visits are coordinated by Kara Lynch (kara.marie.lynch@cern.ch) and she should be contacted well in advance with your wishes.

CERN hostel booking

As for last year, there is a block booking of 20 rooms reserved for visiting ISOLDE experiments. In spite of the change of management of the CERN hostel this has been maintained. However, please note that there is a very strict deadline to be order to reserve these rooms. Rooms must be reserved at least **one month** in advance. After this point, the rooms will be released.

Publications

Please note that ISOLDE should be mentioned in the abstract of articles related to experiments performed at the facility and, if possible, the ISOLDE team should be mentioned in the acknowledgements. Experiments which have benefitted from ENSAR2 funding at ISOLDE should also mention this in the acknowledgements of any articles they publish.

Furthermore, if allowed by the publisher, the phrase "We acknowledge the support of the ISOLDE Collaboration and technical teams" should be used in the acknowledgements and the ISOLDE User Support Office should be informed (via Jennifer.Weterings@cern.ch) when the paper is published

Changes to bike and car rental

CERN continues to offer the possibility of renting bicycles – either for a defined period – or in a daily manner via the "velopass" scheme. In addition, cars are available for users in certain circumstances. 2016 has seen a consolidation of these various services with the opening of a new mobility centre in building 6167 (in the Globe car park) – replacing the previous centre which was located close to the ISOLDE offices. Further details on this and on the procedures to follow in order to rent a bike or car can be found here.

ISOLDE targets and ion sources

Target and Ion Source Development (TISD)

J.P. Ramos, J. Ballof
(for the TISD group)

In 2015, the target and ion source development (TISD) team was expanded with the arrival of four new members: Melanie Delonca as a Fellow and Jochen Ballof, Yisel Martinez and Basil Gonsalves as PhD students. Our main mission is to make beams of new elements and of new exotic isotopes available for physics research. In addition, we make sure that the user community gets the requested beam purity and intensities by tuning and providing the right target and ion source system.

While other developments are on-going (VADIS, LIEBE, nanomaterials and release), in this newsletter we detail two of them in particular: that of the ^{8}B ISOL beam and the developments towards other refractory beams. Furthermore, some words will be spent on the new uranium oxide batch (first used in 2015) and foreseen to be used for the next 20 years, to produce the uranium carbide targets from which 70% of ISOLDE beam time is allocated (on average).

Despite the manifold new developments introduced to ISOL target units within the last 50 years, the extraction of beams from elements with very high melting points (refractory elements) remains still among the most challenging topics [1]. Boron is one of these rebellious elements, which is not only refractory, but also forms stable bonds with various materials the target unit is made of. Motivated by the strong interest from the user community in the ^{8}B ISOL beams, Christoph Seiffert within his PhD thesis, successfully developed and tested a target unit, which allowed the extraction of ^{8}B by in-situ volatilization of boron as fluoride [2]. Sulfur hexafluoride served as fluorinating agent: it was injected through a calibrated gas leak into the target container filled with pressed pills of multiwalled carbon nanotubes. The latter were chosen as target material owing to their favorable diffusion behavior, which was investigated in preparatory experiments. Non-volatile reaction products were trapped in the water cooled transfer line, which connects the target container and the ion source.

Online tests of the prototype unit were conducted in 2014 and 2015. In addition to the tape station, which is equipped with a plastic scintillator and a high-purity germanium detector, an in-beam detection setup was used in LA1, in collaboration with the IDS team. It consisted of a silicon and a high-purity germanium detector (Fig. 1), capable of detecting alpha particles in coincidence with gamma radiation and therefore tailored to the $\alpha 2\beta$+ decay mode of ^{8}B.

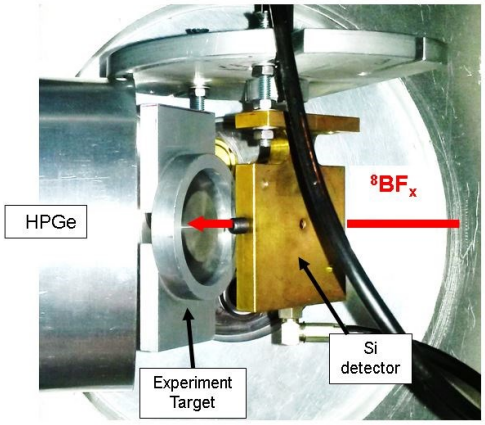

Fig. 1: In-Beam detection setup used for ^{8}B.

As predicted, we were able to measure activity having the signature of ^{8}B on the corresponding masses of $^{8}BF_x$, where x = 0 to 3. In agreement with offline tests, the highest yield was found on the mass of BF_2. It can therefore be concluded, that the ^{8}B beam is now available at ISOLDE and tests for charge breeding and post acceleration are foreseen at HIE-ISOLDE.

As a next step, Jochen Ballof is focusing his PhD project on the remaining blank spots (the refractory elements) of the periodic table shown in Fig. 2, produced from the available ISOLDE beams. A comparison of the blank spot elements with the elements forming volatile carbonyl compounds reveals, that carbonyls seem to be a promising means of transportation for certain refractory elements (cf. Fig. 2). Already in 1970, it was suggested to

extract refractory group 6 - 9 transition metals as carbonyls. [3] However, due to the fragile nature of the compound and other challenges, it was so far not possible to apply this method in ISOL facilities. Due to the low decomposition temperatures of the carbonyl compounds (e.g. 150 °C for $Mo(CO)_6$, [4]), the target must to be kept at relatively low temperatures, in contradiction with the requirement for fast diffusion.

This year, first ionization tests of carbonyl compounds have been conducted at the ISOLDE offline separator. A modified VADIS ion source, which features a cold injection path, and the microwave heated COMIC ion source were tested. After ensuring the reliable ionization, the in-situ reaction of single molybdenum atoms, evaporated from a molybdenum wire, with carbon monoxide gas will be studied. The results of these experiments will yield important information on the requested conditions to form the carbonyl compounds in view of performing more complex TISD tests.

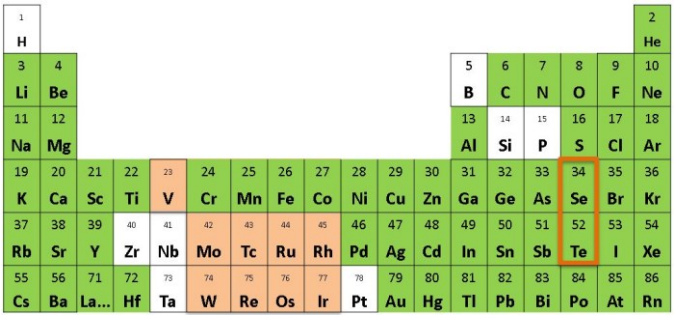

Fig. 2: Elements shown in green are available beams at ISOLDE, orange colored elements are the elements of which no beams are available, but of which carbonyl compounds are known. [5, 6]

The uranium carbide (UC_x) targets at ISOLDE are produced by mixing uranium oxide (UO_2) and graphite powders. The mixture is pressed into powder compacts ("pellets") and heated in vacuum up to 2000°C, to promote the carbothermal reduction of UO_2 into UC_x (with excess graphite), where x is between 1 and 2 - UC and UC_2 phases obtained. For the last 10 years at ISOLDE, UC_x targets were produced using the same 10 kg UO_2 batch. In the beginning of 2015 the last targets from this batch were produced and a new one had to be obtained.

Westinghouse supplied us with a new UO_2 batch of 20 kg with very few differences in chemical impurities when compared with the old one, as given by the supplier. The targets from this new batch have shown systematically high and stable yields over time (see example on Fig. 3). Furthermore, being operated at conservative temperatures, these targets have provided beams of (exotic) isotopes, that matched and even surpassed, in some cases, database record yields. [7]

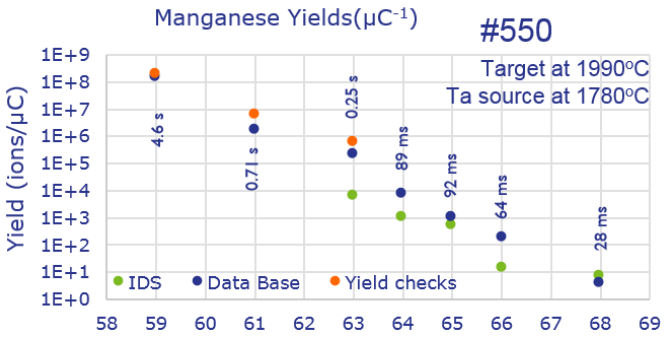

Fig. 3: Manganese yields extracted from the new uranium carbide targets coupled with a tantalum surface ion source.

With such an interesting new UO_2 batch, ISOLDE has much to gain, since UC_x targets are used for >70% of the beam time at ISOLDE. From the R&D point of view we are very interested in studying this new material and compare it to the old one, to unveil the differences. This will surely shine some more light into the target material characteristics influencing the complex isotope release processes. In the long run we wonder how much the new UO_2 batch will impact the isotope production from the nanoUCx [8], a target that has revealed promising results already.

This year, we are excited to test online a few targets which include another negative ion source, a carbon surface ion source (developed by S. Rothe from the RILIS team) and an iteration of the nanoUCx produced with the new UO2 batch. Furthermore, we will also test the LIEBE target prototype, realized with a large collaboration: for more information please read the ISOLDE Newsletter from 2014 and 2015.

[1] U. Köster et. al., Eur. Phys. J. Special Topics 150, 285–291 (2007).
[2] C. Seiffert, PhD Thesis, Technische Universität Darmstadt, 2015.
[3] K. Baechmann. Chemical Problems of the On-Line Separation of Short-Lived Nuclides. Forschungsbericht K70-28, BMBK-FB-L70-28, 1970.
[4] R. C. Weast (Editor), CRC Handbook of Chemistry and Physics (Boca Raton), 64th Edition, 1983-1884.
[5] Isolde yield database, http://test-isolde-yields.web.cern.ch, retrieved on 03/10/2016.
[6] C. Elschenbroich, Organometall-chemie (Teubner), 6th Edition, 2008.
[7] J.P. Ramos, ISOLDE Workshop and Users meeting 2015 (Oral Contribution), http://cern.ch/go/6fL9

[8] A. Gottberg, et al., in preparation.

A new scheme: RILIS ionized tellurium at ISOLDE

ISOLDE-RILIS
Website: http://rilis.web.cern.ch

Thomas Day Goodacre
(for RILIS)

Following recent RILIS beam development work, tellurium can now be added to the list of elements available for ionization by the ISOLDE-RILIS [1]. A consequence of the element selective RILIS method of ionization [2], is that a multistep resonance photo-excitation "scheme" must be investigated for each element of interest. The priorities for RILIS scheme development are based upon feasibility and the priorities set by the INTC and the GUI (Group for the Upgrade of ISOLDE). Requests for new schemes typically go via the ISOLDE physics coordinator. The development of RILIS ionized tellurium ion beams at ISOLDE was triggered following a request by the IS516 Coulomb excitation of ^{116}Te and ^{118}Te experiment [3].

While not for ISOLDE beam production, laser resonance ionization of tellurium had been applied previously at ISOLDE in a COMPLIS experiment, where a three-step scheme with a non-resonant final excitation step with 1064 nm photons was used ($\{\lambda_1, \lambda_2, \lambda_3\}$ = {214.35, 591.53, 1064^{NR}} (vacuum wavelengths)) [4]. As the experiment did not involve ionization inside a hot cavity, there were no measured efficiencies applicable to the RILIS. A rich continuum of autoionizing states of tellurium was identified in the 1980s using flash pyrolysis and other non-laser light sources [5-7]. Autoionizing resonances of tellurium have also been investigated at Oak Ridge National Laboratory (private communication Y. Liu).

The new RILIS scheme for tellurium was developed opportunistically during the 2015 spring start-up of ISOLDE. The transitions are presented in Fig. 1, details of the scheme development can be found in [1]. The new scheme makes full use of the flexibility offered by the dual Dye-Ti:Sa laser system installed at the ISOLDE-RILIS [8]. It was found to be >2.5 times more efficient than alternative schemes using the available second excitation steps (λ_2) followed by non-resonant ionization with 532 nm photons {214.28, λ_2, 532^{NR}}, despite the fact that the 532 nm laser beam was ~25 times more powerful than the one used for the autoionizing transition employed in the scheme depicted in Fig 1.

An efficiency measurement was possible during the 2016 spring start-up, as part of the "cold checkout" verification of the RILIS systems for the 2016 on-line period. The RILIS lasers were directed into a hot cavity ion source mounted on the GPS front-end, while a calibrated 1000 nAh mass marker of stable tellurium was evaporated and the ion current measured with a Faraday cup located downstream of the separator magnet. An efficiency of >18% was measured. This value is the combined efficiency of extraction, ionization and beam transport to the first Faraday cup after the GPS magnet (FC490). The efficiency compares favorably with the other RILIS scheme efficiencies measured at ISOLDE.

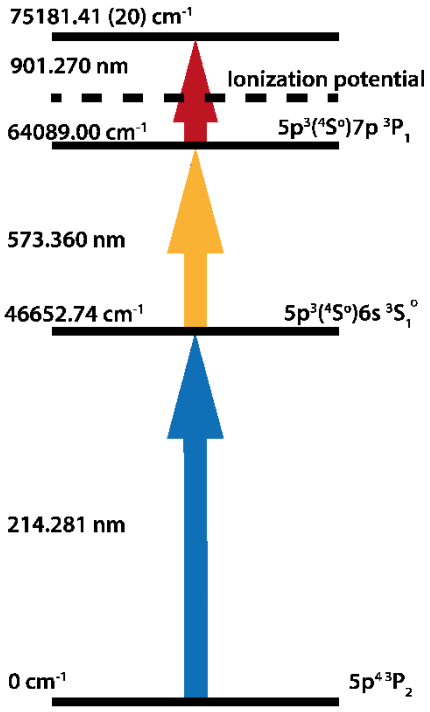

Fig. 1: The new RILIS ionization scheme for tellurium, taken from [1].

[1] T. Day Goodacre et al. (2016) NIMA, (In Press) http://dx.doi.org/10.1016/j.nima.2015.10.066
[2] V. I. Mishin et al. (1993) NIMB, 73, (4) pp. 550-650 http://dx.doi.org/10.1016/0168-583X(93)95839-W
[3] T. Ahn et al. (2011) CERN-INTC, IS516, http://cds.cern.ch/record/1319097
[4] R. Sifi et al. (2006) Hyperfine interactions 171, (1-3) pp. 173-179 http://dx.doi.org/10.1007/s10751-006-9505-0
[5] J. Berkowitz et al. (1981) Phys. Rev. A. 24, pp.149-160 http://dx.doi.org/10.1103/PhysRevA.24.149

[6] A. M. Cantú et al. (1983) Physica Scripta 27 (4) 261-266 http://dx.doi.org/10.1088/0031-8949/27/4/007
[7] M Mazzoni et al. (1983) J. Phys. B: At. Mol. Phys. 16 pp. 3183-3190 http://dx.doi.org/10.1088/0022-3700/16/17/011
[8] S. Rothe et al. (2011) J. Phys.: Conf. Ser. 312 052020 http://dx.doi.org/10.1088/1742-6596/312/5/052020

VADLIS: elements selective RILIS ionization in an ISOLDE VADIS

ISOLDE ion source development
Website: http://rilis.web.cern.ch

Thomas Day Goodacre
(for ISBM)

The RILIS (Resonance Ionization Laser Ion Source) [1, 2] is the primary ion source of the ISOLDE facility, requested for >70 % of the beam time for experiments and LOIs in the first half of 2016. The possible application of the RILIS has been extended following its successful demonstration inside the anode cavity of a VADIS (Versatile Arc Discharge Ion Source) [3], ISOLDE's latest variant of the FEBIAD type ion source [4]. Recent on-line and off-line characterization and results of the new ion source combination, termed the VADLIS (Versatile Arc Discharge and Laser Ion Source), are summarized in the upcoming proceedings of the 2015 EMIS conference published in NIMB [5].

By operating the VADIS with an anode voltage in the region of 2-10 V, a comparably efficient but element selective RILIS-mode of operation has been determined. A schematic depicting the VADLIS operation is presented in Fig. 1.

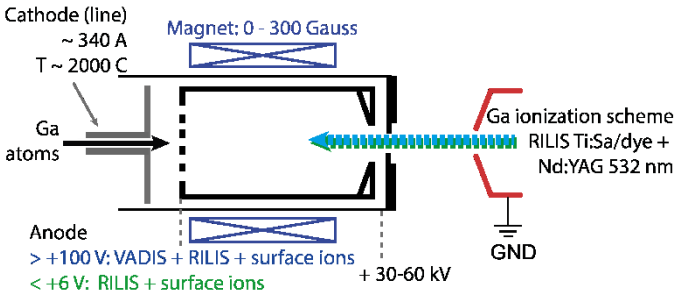

Fig. 1: Schematic of the VADLIS Ion source, taken from [5]

During the 2015 on-line period, the RILIS-mode was applied for the IS598 in-source laser spectroscopy of mercury experiment [6]. Further on-line testing took place using the RILIS lasers to ionize cadmium in a VADIS coupled to a molten tin target. The relative efficiencies for ^{178}Hg and ^{114}Cd are presented in Fig. 2.

For RILIS ionizable beams [7], the demonstrated VADLIS capabilities offers Users at ISOLDE a number of new options when a VADIS ion source is coupled to a target.

- Element-selective ionization, which in specific cases (such as mercury) could be also isomer-selective.
- Signal identfication through laser on/off measurements, as is standard procedure for hot cavity RILIS operation.

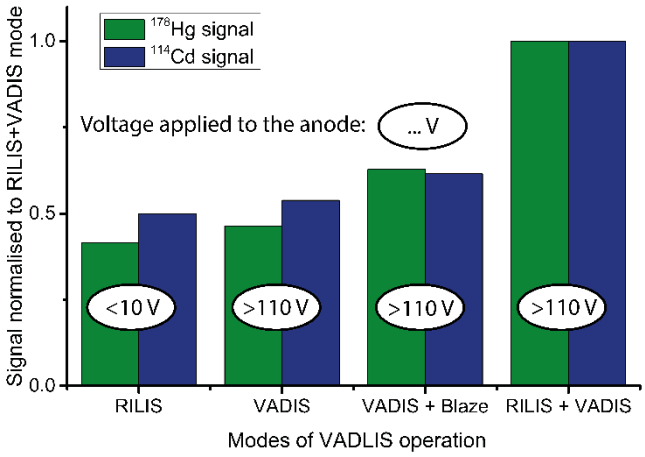

Fig. 2: VADLIS modes of operation, taken from [5]. The Blaze is a 40 W laser typically applied as a non-resonant final step for certain RILIS schemes.

- An efficiency boost without additional heating/faster degredation of the ion source.
- RILIS coupled with molten metal targets at ISOLDE.

Promising RILIS-mode selectivity has been observed for barium compared to hot cavity RILIS operation, however, the efficiency has yet to be determined.

Characterization and development is ongoing under the framework of the ISOLDE Ion Sources and Beam Manipulation working group (ISBM). It is hoped these results represent just the beginning of new applications and optimization.

[1] V.N. Fedosseev et al. (2012) Rev. Sci. Instrum. 83, 02A903. http://dx.doi.org/10.1063/1.3662206
[2] S. Rothe et al. (in press) NIMB.

http://dx.doi.org/10.1016/j.nimb.2016.02.024
[3] L. Penescu et al. (2010) Rev. Sci. Instrum. 81, (2):02A906. http://dx.doi.org/10.1063/1.3271245
[4] R. Kirchner and E. Roeckl. (1976) NIM 133(2):187–204. http://dx.doi.org/10.1016/0029-554X(76)90607-8
[5] T. Day Goodacre et al. (in press) NIMB. http://dx.doi.org/10.1016/j.nimb.2016.03.005
[6] L.P. Gaffney et al. (2014) CERN INTC, (P-424). https://cds.cern.ch/record/1953719
[7] RILIS elements database. http://riliselements.web.cern.ch

HIE-ISOLDE project

HIE-ISOLDE Phase1

Y. Kadi and W. Venturini Delsolaro

The first cryomodule of the new superconducting linear accelerator HIE-ISOLDE (High Intensity and Energy ISOLDE), located downstream of the REX-ISOLDE accelerator, was successfully installed and commissioned last year, increasing the energy of the radioactive ion beams from 3 to 4.3 MeV per nucleon. It supplied the Miniball array, with radioactive zinc ions until the end of the proton run in November 2015.

Fig. 1: Assembly of the first HIE-ISOLDE cryomodule, with its five copper cavities in the new SM18 cleanroom (http://cds.cern.ch/record/2007275).

This is the first stage in the commissioning of HIE-ISOLDE. The facility will ultimately be equipped with four cryomodules that will accelerate the beams to 10 MeV per nucleon and increase their intensity fourfold. Each cryomodule has five accelerating cavities and a solenoid, which focuses the beam. All of these components are superconducting.

This first beam is the result of eight years of development and manufacturing. One of the major challenges was the construction of the cavities. The HIE-ISOLDE cavities are made of copper coated with a thin layer of niobium, a superconducting material. This technology, which had been used for the LEP and then for the LHC, had to be adapted to the more complex geometry of a quarter-wave cavity. To date, twelve cavities have been qualified and will be installed at a later stage.

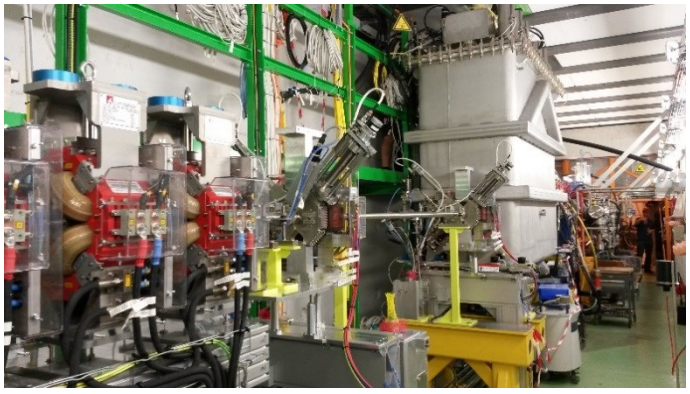

Fig. 2: The first HIE-ISOLDE cryomodule can be seen in the background, in its light-grey cryostat

Assembling the cryomodule also presented a challenge. Unlike the LHC cryomodules, for example, in which the internal surfaces of the cavities are isolated from the other components, all the elements of the HIE-ISOLDE cryomodule are located in the same vacuum. The cryomodule is therefore more compact, which is essential given the limited space in the ISOLDE building. Materials have been specially chosen to ensure that the components can be perfectly cleaned and that the quality of the vacuum is not degraded while the machine is running. A class ISO5 cleanroom was purpose-built for the assembly of the cryomodules.

After a delicate assembly phase in the cleanroom, the first cryomodule was transported to the ISOLDE hall on 2 May 2015 and coupled to the existing REX-ISOLDE accelerator. The commissioning began in the summer, and was followed in September 2015 by the first tests, culminating in the acceleration of the first radioactive beam on 22 October 2015. HIE-ISOLDE ran for a total of five weeks last year as detailed next.

During this technical stop, another cryomodule will be coupled to the first, increasing the energy to 5.5 MeV per nucleon. Two other cryomodules will be installed from mid-2017 onwards, bringing the final energy to 10 MeV per nucleon for the heaviest nuclei generally produced at ISOLDE.

Beam Commissioning and Operations of REX/HIE-ISOLDE

J. A. Rodriguez Rodriguez

The beam commissioning of the post-accelerator started in June 2015 after the refurbishment of the REX normal conducting linac was completed. Three different pilot beams produced in the EBIS were used during this time ($^{12}C^{4+}$ with A/Q = 3.0, $^{14}N^{4+}$ with A/Q = 3.5 and a mixture of $^{20}Ne^{5+}$, $^{16}O^{4+}$ and $^{12}C^{3+}$ with A/Q = 4.0).

The beam commissioning was divided into different stages. First, beam accelerated to 0.3 MeV/u was used to re-commission the REX diagnostics box (Fig. 3) after the operational settings of the RFQ were determined. Second, beam with that same energy (all other RF structures were turned off) was transported to the first HIE-ISOLDE diagnostics box and used to commission the Faraday cup, the silicon detector and the scanning slits.

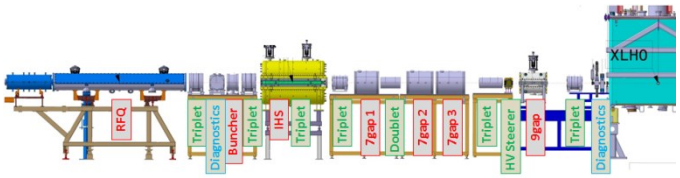

Fig. 3: Layout of the REX normal conducting linac

Third, the silicon detector was used to determine the needed RF power out of the amplifiers and to phase each of the accelerating structures. The velocity at the exit of each normal conducting cavity is the same for every ion. Therefore, the relative phases for the cavities do not change and it is not necessary to re-phase the cavities. However, the RF reference line was replaced during the refurbishment of the RF systems of the linac making it necessary to re-phase all the cavities at this time.

Fourth, beam with the REX nominal energy was drifted through the cryomodule while the superconducting cavities were off. This beam was used to commission the diagnostics and the optical elements of the linac and the first High Energy Beam Transfer (HEBT) line (Fig. 4).

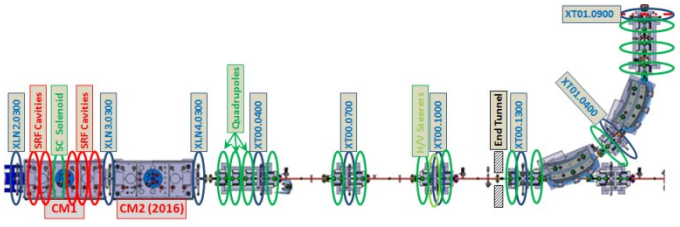

Fig. 4: Layout of Phase 1 of the HIE-ISOLDE linac and the first experimental line

Fifth, the superconducting cavities were commissioned and phased using a Si detector in a diagnostics box at the end of the tunnel. Beam was transported along the second HEBT line and the different elements of the line were tested during the last stage of the beam commissioning.

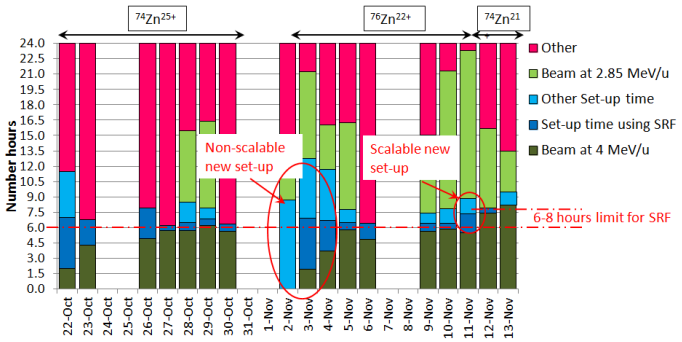

Fig. 5: Beam time available to users during the first HIE-ISOLDE physics experiment in green. Time spent setting up the machine in blue.

Operations started in mid-October with preparations for the delivery of beam to users. Before the physics campaign started and in order to test the accelerator chain, stable ^{87}Rb beam was produced in the GPS target, accumulated and cooled in the TRAP, charge-bred to $^{87}Rb^{28+}$ in the EBIS and accelerated to 2.85 MeV/u in the REX normal conducting linac. In addition, stable $^{12}C^{4+}$ produced in the EBIS, was used as a pilot beam to phase the superconducting cavities and to set up the HEBT lines.

On October 19th, the first experiment of the campaign started with the delivery of stable $^{22}Ne^{7+}$ with an energy of 2.85 MeV/u to the Miniball experimental station. The first 4 MeV/u radioactive beam was delivered a few days later on October 22nd. Over the following weeks, different charge states of two zinc isotopes ($^{74}Zn^{25+}$, $^{76}Zn^{22+}$ and $^{74}Zn^{21+}$) and energies of 2.85 and 4 MeV/u were sent to the experimental station (Fig. 5). The 4 MeV/u beam was limited to 6-8 hours per day due to the overheating problem of the couplers of the superconducting cavities. Beam with the final energy of the normal conducting linac was used during the rest of the time.

In addition to the radioactive Zn to the Miniball experimental station, several stable beams were delivered to the scattering chamber (a few hours of $^{14}N^{4+}$ and $^{12}C^{4+}$ beams) and to the SPEDE detector (4.5 days of $^{133}Cs^{39+}$ beam) for commissioning purposes.

Cryomodule Assembly Activities

Y. Leclercq

On 8 January 2016, the first high-β cryomodule (CM1) was transported from the ISOLDE facility back to the dedicated clean room in SM18 for refurbishment. During commissioning in the summer of 2015, it was found that the performance of the RF superconductive cavities was limited by the over-heating of their RF couplers. The decision was taken to launch the design of a coupler heat extraction system. In record time, the problem was identified, the design completed and parts were manufactured and installed in the second cryomodule (CM2) being assembled in the clean room.

Fig. 6: Final verifications on Cryomodule #2 before closure and transport to the ISOLDE facility.

The upgraded assembly of CM2 was completed at the end of February 2016 (see figure 6) and directly transported onto the ISOLDE beam line. As soon as the clean room was made available, CM1 was inserted and its refurbishment started.

Following the opening of the cryomodule, under guidance of the radioprotection service, a detailed health check of all internal components was carried out after a thermal cycle to 4.5K, the first physics run and transport to and from the ISOLDE beam line. Causes of all performance issues raised during the commissioning were found and diagnostics confirmed. The refurbishment could then start with the disassembly of the RF cables and couplers as well as the disassembly of one cavity (referred to as CAV#2) that was sent for rinsing to lower its level of observed field emission. Once rinsed and conditioned, the cavity returned to the clean room, was prepared and inserted into the cryomodule (see figure 7). The new couplers were installed along with their improved heat extraction systems allowing the start of the closing procedure on 8 March 2016. At the time of writing, all final tests are positive; the leak test did not reveal leaks above 1.10^{-10} mbar.l.s^{-1} and RF tests were positive and completed by mid-March. The final survey operation should confirm the alignment of the superconducting components within ±0.3mm and CM1 should be closed again by the end of March. After two weeks of final tests outside of the clean room, CM1 will be transported under vacuum and returned to its place on the ISOLDE beam line.

Fig. 7: Installation of instrumentation on the rinsed superconductive cavity before assembly into CM1.

In parallel with the commissioning of CM1 and CM2 in the ISOLDE facility, the assembly of the final two high–β cryomodules (CM3 and CM4) for the phase 2 of the HIE-ISOLDE upgrade will take place. All cryostat components for these units are now at CERN and their preparation, verification, and reception tests have been underway since early February in SMA18. All staff are intensely involved in this preparation for assembly of CM3 in the clean-room. All parts from the smallest screw to the vacuum vessel weighing 3.5 tons are mechanically verified, leak tested or surveyed when esteemed needed and thoroughly cleaned to UHV standards. In addition, assembly procedures and mechanical drawings are being reviewed and upgraded to ensure a smooth, efficient and optimized assembly in the clean room. CM3 is expected to be transported to the beam line by the end of the year, after the physics run.

HIE-ISOLDE Installation Works

E. Siesling

During the shutdown of 2016, as part of Phase 1b, the second Cryomodule has been added to the SC Linac which will increase the total energy of the beam to 5.5 MeV/u. Earlier this year the first cryomodule was disconnected in the shielding tunnel from all its services (vacuum, RF and cryogenics) and has been shipped back to the cleanroom in SM18 for retro-fitting of the RF couplers.

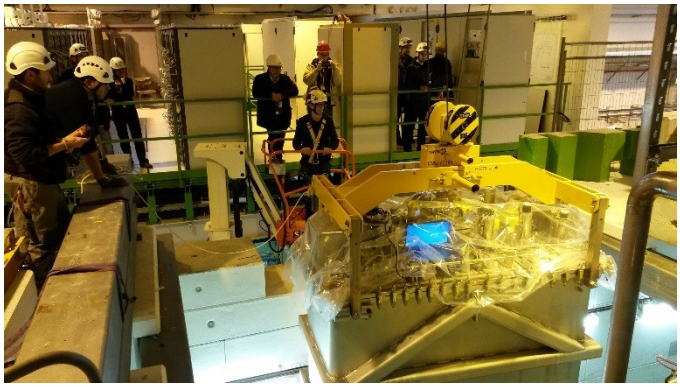

Fig. 8: Dismounting Cryo Module 1 in the HIE shielding tunnel for retro fitting of the coupler in SM18

Fig. 9: Arrival of Cryomodule 2 by truck from SM18

CM1 will be installed back in the HIE-ISOLDE shielding tunnel by mid-April. As far as the installation is concerned, we are on track with regard to the schedule. The second cryomodule, CM2, has been installed inside the tunnel, aligned and the downstream vacuum chambers connected as well as the intertank sector which holds a corrector magnet as well as a beam instrumentation diagnostic box. A high tech BCAM camera observation system is installed at the intertank position on both sides of each cryomodule which looks into the vessel to measure and verify at all times the exact position of the cavities and solenoid with respect to the beam axis.

Fig. 10: Cryomodule 2 being connected to its services in the HIE-ISOLDE shielding tunnel

The vacuum system for CM2 has been connected as well as all the top plate services as we speak: RF cabling, motor control and instrumentation cabling and cryogenic connections from the cryomodule to the cryo jumper box outside the tunnel to feed the Module with liquid Helium and cooldown the Nb sputtered Super Conducting cavities and solenoid to an operational temperature of 4.5K.

The Cryogenic plant maintenance and connections to the two cryomodules will finish end of April, in time to start the cooldown of both cryomodules for the Hardware- and Beam-Commissioning at the beginning of May 2016. Physics with 5.5MeV/u Radioactive Ion Beams is expected to start this summer serving both the Miniball and Scattering Chamber experiments which are installed on the XT01 and XT02 High Energy Beam Transfer lines respectively.

HIE-ISOLDE Planning for 2016

F. Formenti

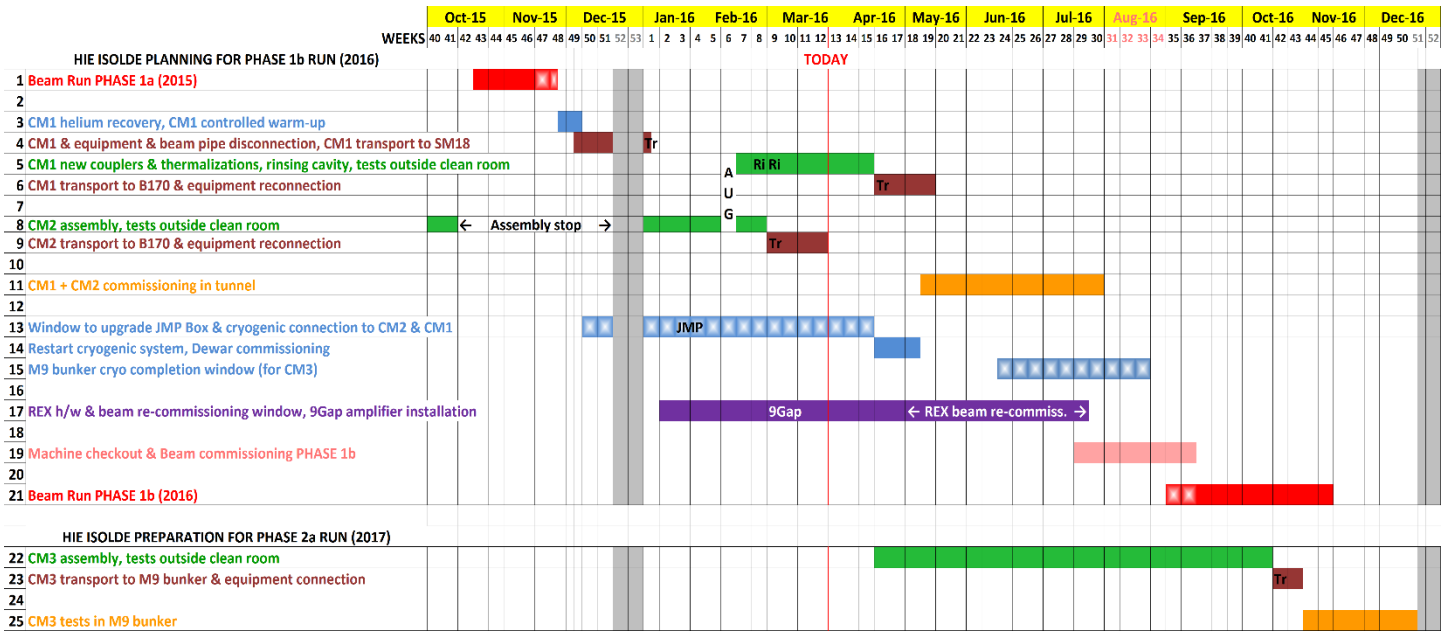

Fig. 11: Planning for beam run with two Cryomodules (Phase 1b) and preparation of CM3 (Phase 2a).

2015 marked the successful start of the HIE-ISOLDE linear accelerator with the first accelerating structure consisting of 5 superconducting cavities installed in the first Cryomodule (CM1). In this configuration, identified as Phase 1a, the accelerator could supply 5.5 weeks of beam, as from week 43/2015 to mid week 48/2015.

The assembly of the second Cryomodule (CM2), which was already initiated in the summer of 2015, required a sudden stop at the end of week 41/2015 because of an unexpected overheating problem of one RF coupler.

The CM2 assembly could only restart at the beginning of 2016, after 10 weeks of intense work for the identification of the corrective action and the urgent supply of the new parts. CM2 assembly was completed in week 5/2016, well within the remaining 5 weeks of the original assembly roadmap plan.

Following the end of the beam run Phase 1a, CM1 was warmed up, disconnected and transported, in week 1/2016, to SM18 waiting for accessing the assembly clean room and undergoing the same consolidation of its couplers and for rinsing of one of the cavities.

Since the end of the CM1 warm up, in week 50/2015 the cryogenic system entered the upgrade period for cooling down two Cryomodules. It will be restarted to provide liquid helium to both of Cryomodules by the end of week 18/2016.

In wk19/2016 CM1 and CM2 will be fully connected to the services, aligned and ready to be operated during the next phase of hardware commissioning. This phase is planned to last 12 weeks, until week 30/2016.

In parallel to what is described in the two paragraphs above, also the Rex accelerator will be re-commissioned and the test beam will be injected up to the dump which is just in front of the first Cryomodule.

In the new configuration with two Cryomodules, identified as Phase 1, the HIE linac will supply beam to two experimental lines, during 2 weeks of beam start-up and 9 weeks of physics. This is scheduled as from week 35/2016 until the end of the 2016 proton run.

The assembly of the third Cryomodule (CM3) can start week 16/2016, as soon as CM1 has left the clean room. It will be performed in parallel to the commissioning of CM1 and CM2 and terminated while supplying beam during the Phase 1b. The test of CM3 will initially be performed in the M9 bunker and then completed in the linac facility in 2017 (Phase 2a, with three Cryomodules).

RIB applications to medical and solid-state physics

Alpha-PET with ^{149}Tb: Evidence and Perspectives for Radiotheragnostics

Results of experiment IS528

N. van der Meulen, C. Vermeulen, K. Johnson, U. Köster, C. Müller

^{149}Tb is an attractive radionuclide for targeted α-therapy in combination with small molecules, due to its favourable half-life of 4.1 h and the absence of α-particle emitting daughter radionuclides [1,2]. The possibility of stable coordination using DOTA (1,4,7,10-tetraazacyclododecane-1,4,7,10-tetraacetic acid: a chelator for stable linking of trivalent metals) allows its use with conventional targeting agents previously established in combination with ^{177}Lu [3]. In addition to α-emission, ^{149}Tb also emits positrons ($I_{\beta+}$=7.1%). In this study the potential of ^{149}Tb for PET imaging in mice, using a well-established somatostatin analogue, was investigated [4].

^{149}Tb was produced at ISOLDE. To enhance the usable terbium activity, the dysprosium (Dy) isobars of the isotopes of interest were laser-ionised and collected in a Zn-coated Au foil, the creation of terbium taking place directly in the sample by electron capture decay. The ^{149}Tb yields and beam purity were optimized by on-line measurements of the beam composition with the ISOLTRAP MR-TOF-MS [5].

The implanted foils were shipped to Paul Scherrer Institut for chemical separation. The radionuclides were dissolved in HNO_3/NH_4NO_3, loaded onto a macroporous cation exchange resin and the ^{149}Tb eluted using dilute α-hydroxyisobutyric acid (α-HIBA). A quantity of ~100 MBq ^{149}Tb was effectively separated from impurities, yielding a radionuclidically pure product. The product eluent was used directly for the radiolabelling of DOTANOC.

NOC is a somatostatin analogue (a peptide) that selectively targets neuroendocrine tumours. ^{68}Ga- and ^{177}Lu-labelled somatostatin analogues are already in clinical use for molecular imaging and radionuclide therapy of neuroendocrine tumours, respectively [6,7].

The radiolabelling process produced ^{149}Tb-DOTANOC at a specific activity of 10 MBq/nmol and a radiochemical purity of >96%. Female nude mice with AR42J tumours were injected with ^{149}Tb-DOTANOC (7 MBq). PET/CT imaging studies were carried out 1 h and 2 h after injection using a G8 bench-top scanner (Sofie Biosciences). Visualisation of tumours using PET/CT was readily possible in mice injected with ^{149}Tb-DOTANOC (Fig. 1). In non-targeted tissue, radioactivity accumulation was only observed in the kidneys as a consequence of renal excretion of the radiopeptide.

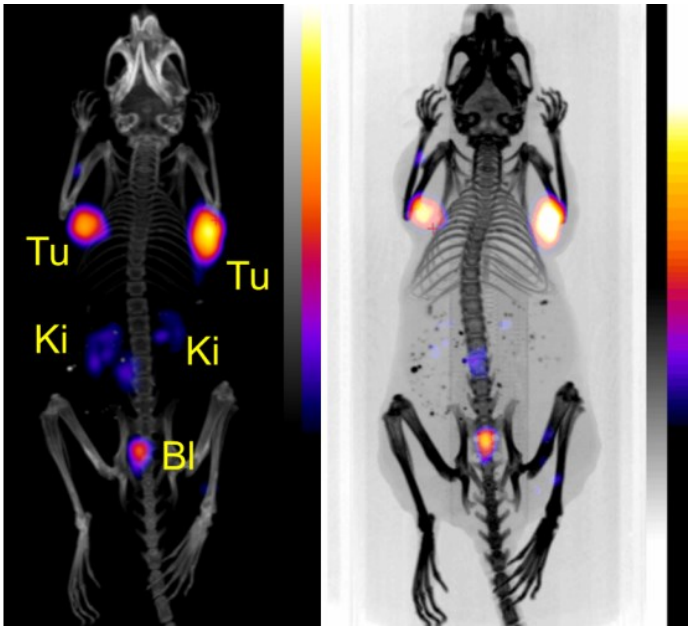

Fig. 1: PET/CT images of an AR42J tumour-bearing mouse 2 h after injection of 149Tb-DOTANOC (7 MBq). The images showed distinct accumulation of radioactivity in tumour xenografts (Tu) and residual radioactivity in kidneys (Ki) and the urinary bladder (Bl).

In this study, ^{149}Tb was successfully employed for in vivo PET imaging. These results were achieved due to the excellent quality of the ^{149}Tb produced, allowing

radiolabelling of DOTANOC at high specific activity and also due to the high sensitivity of the PET scanner.

This radiotheragnostic application using α-PET imaging is a unique feature to ^{149}Tb: none of the other clinically useful α-emitters permit PET imaging. The next IS528 beam schedule will be used to investigate the theragnostic properties of ^{149}Tb further.

We are grateful to the ISOLDE RILIS team for reliable Dy ionization and to the ISOLTRAP MR-TOF-MS team for rapid on-line analysis of the beam composition.

[1] G.J. Beyer et al., Eur. J. Nucl. Med. Mol. Imaging 31, 547 (2004).
[2] C. Müller et al., J. Nucl. Med. 53, 1951 (2012).
[3] C. Müller et al., Pharmaceuticals 7, 353 (2014).
[4] C. Müller et al., EJNMMI Radiopharm. Chem. 1, 5 (2016).
[5] S. Kreim et al., Nucl. Instrum. Meth. B 317, 492 (2013).
[6] D. Wild et al., J. Nucl. Med. 54, 364 (2013).
[7] R.P. Baum et al., Theranostics 6, 501 (2016).

A radioactive ion's view on artificial multiferroics

Results of experiment IS580

Valérie Augustyns and Lino Pereira
(for the Emission Channeling collaboration)

Multiferroic materials exhibit at least two ferroic order parameters. Magnetoelectric multiferroics, in particular, combine ferroelectricity and (anti)ferromagnetism. The interest in these systems derives from the coexistence of electric and magnetic order parameters and, in fewer though more interesting cases, from the magnetoelectric coupling between them. However, the long-sought multiferroic with large magnetoelectric coupling above room temperature remains to be discovered. An alternative to intrinsic multiferroics, particularly for magnetoelectric coupling as a means of electric control of magnetism, is to combine ferroelectric and ferromagnetic materials in hybrid systems, known as *artificial multiferroics*, such as multilayers and embedded nanostructures. One of the main advantages of this approach is the much wider range of materials exhibiting ferroelectricity or ferromagnetism, even above room temperature.

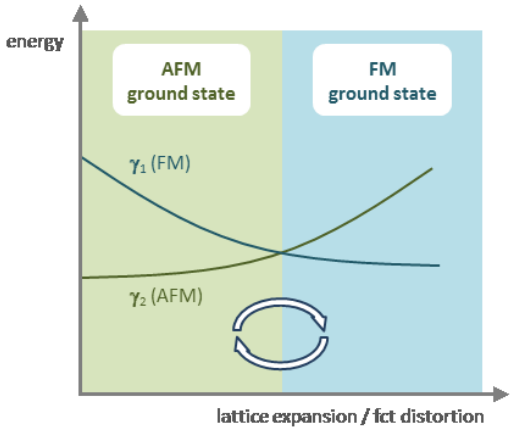

Fig. 1: Principle of the magnetoelectric coupling mechanism in our model system (γ-Fe nanoparticles embedded in $SrTiO_3$).

Our work deals with the realization of a new type of magnetoelectric coupling in artificial multiferroics, in which strain induced by a ferroelectric host drives the magnetic material (with which it is interfaced) between different magnetic ground states. Our model system consists of γ-Fe nanoparticles embedded in a $SrTiO_3$ matrix (prepared by ion implantation of Fe into $SrTiO_3$),where the γ-Fe nanoparticles can be switched between ferromagnetic (FM) and antiferromagnetic (AFM) ground states (γ_1 and γ_2 in Fig. 1) upon strain-induced lattice distortion.

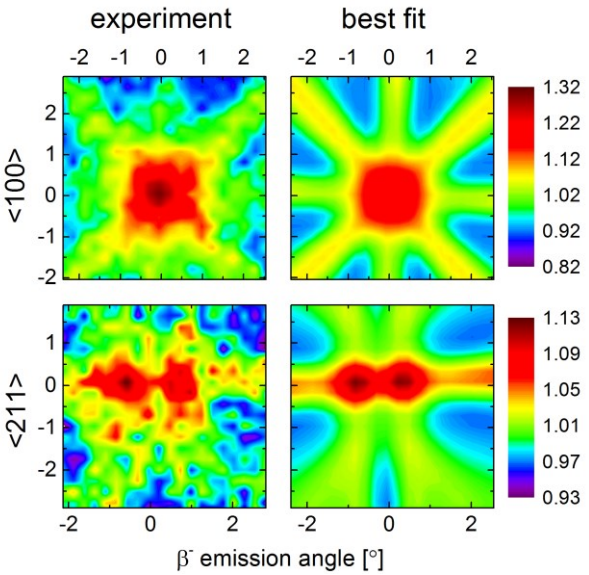

Fig. 2: (*Left*) Experimental ^{59}Fe β$^-$ emission channeling patterns in the vicinity of the <100> and <211> directions. (*Right*) Corresponding best fits yielding 26(6)% of the Fe atoms in Ti sites, and the remaining 73(5)% contributing with an isotropic emission (corresponding to ^{59}Fe in γ-Fe nanoparticles).

Our work is based on a combination of various experimental methods, involving conventional techniques (e.g. SQUID magnetometry and transmission electron microscopy) as well as techniques available in large-scale facilities (e.g. emission channeling at ISOLDE, and X-ray diffraction and X-ray absorption fine structure at the European synchrotron ESRF). Emission channeling plays a crucial role by probing the atomic configuration of the Fe atoms which do not segregate in γ-Fe nanoparticles but, instead, occupy Ti sites in a random $SrTi_{1-x}Fe_xO_3$ alloy (Fig. 2). Samples are first implanted with stable ^{56}Fe with fluences in the range of 10^{15}-10^{16} atoms per cm^2 and subsequently co-implanted at ISOLDE with ^{59}Mn ($t_{1/2}$ = 4.6 s), with fluences of the order of 10^{12} atoms per cm^2. The precursor isotope ^{59}Mn, decays to ^{59}Fe ($t_{1/2}$ = 46 days). The β^- emission channeling spectra (Fig. 2) are measured upon decay of ^{59}Fe to stable ^{59}Co. The insight provided by emission channeling helps us understand not only the mechanism of Fe segregation into γ-Fe nanoparticles, but also how the Ti-Fe alloying, i.e. the dilute Fe component, induces biaxial strain on the $SrTi_{1-x}Fe_xO_3$ layer in which the γ-Fe nanoparticles are embedded.

News from the Mössbauer collaboration

IS501, IS576, IS578 & I161
Website: http://e-ms.web.cern.ch/

Haraldur Páll Gunnlaugsson and Torben E. Mølholt (for the Mössbauer collaboration at ISOLDE/CERN)

2015 was again a successful year for the Mössbauer collaboration at ISOLDE/CERN, where several new beams were utilized for both on-line and off-line emission Mössbauer spectroscopy. For the first time, we received laser ionized ^{119}In ($T_{½}$ = 2.1 min.) during our May on-line beam-time, which resulted in 20 times higher count-rate than previously received using surface ionization only. Instead of collecting data for hours, we obtained high statistics emission spectra within minutes. This allowed us to perform more difficult and diverse measurements which would have been otherwise impossible [1].

Additionally an off-line Mössbauer laboratory has been set up in building 508 (on loan from Aarhus University), where it is now possible to perform research making use of longer lived parent isotopes for emission Mössbauer spectroscopy. The new laboratory was used for samples implanted with $^{151}Dy \rightarrow {}^{151}Gd$ ($T_{½}$ = 120 d) and it turned out that ISOLDE could produce samples with sufficient activity within minutes. This demonstrates that we have a new useful isotope of interest for solid state physics. An example is shown in Fig. 1.

IKS in Leuven provided us with a cryostat, where it is possible to measure isotopes with rather high energy Mössbauer transitions (>50 keV). This facility (see Fig. 2) will eventually allow us to make use of most of the documented Mössbauer isotope transitions.

Although the setup was not fully put in operation at 4.2 K, it was however possible to perform test and feasibility experiments at 77 K to demonstrate that the system works (Fig. 3) using the 77.3 keV Mössbauer transition of $^{197}Au(\leftarrow{}^{197}Hg)$. It will be ready for biophysics experiments later this year.

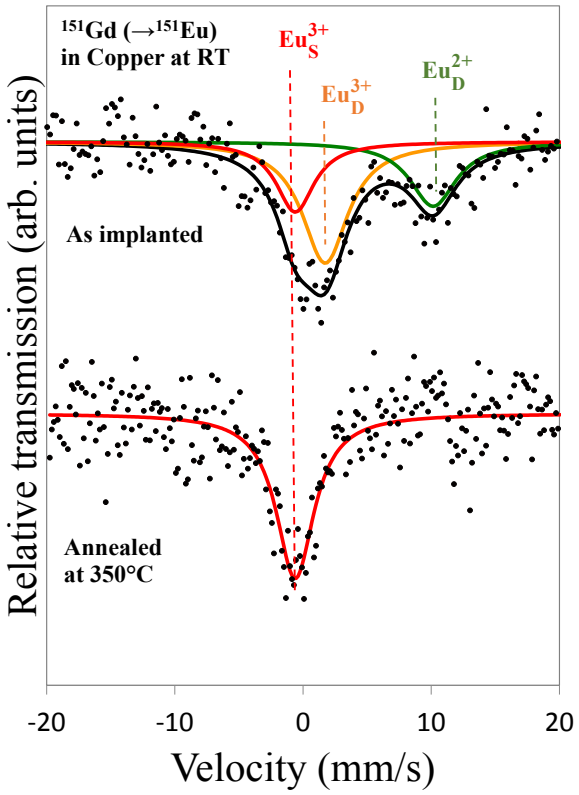

Fig. 1: ^{151}Eu emission Mössbauer spectra obtained after implantation of ^{151}Dy into copper, before and after annealing. Before annealing, ^{151}Eu is found in both 2+ and 3+ damage sites. After annealing, only narrow line due to Eu^{3+} on crystalline sites remains.

Fig. 2: The IKS cryostat during testing. The Mössbauer drive system is on top of the cryostat, and the detector below.

Tantalum has a higher Debye temperature than Au which is seen in the deeper spectral absorption in Fig. 3. The position of the resonances is in accordance with data from the literature.

The interest in emission Mössbauer spectroscopy is still increasing. At the February INTC meeting, two new proposals were submitted that include emission Mössbauer spectroscopy: “Study of molybdenum oxide by means of Perturbed Angular Correlations and Mössbauer spectroscopy” by Juliana Schell and “Unraveling the local structure of topological crystalline insulators using hyperfine interactions” by Lino Pereira.

The next team meeting/workshop of the Mössbauer collaboration at ISOLDE/CERN, WEMS2016 [2], will be held from 30 June to 2 July 2016 as a satellite meeting to the International conference on Hyperfine interactions and their Applications [3] held in Leuven, Belgium July 3-8, 2016.

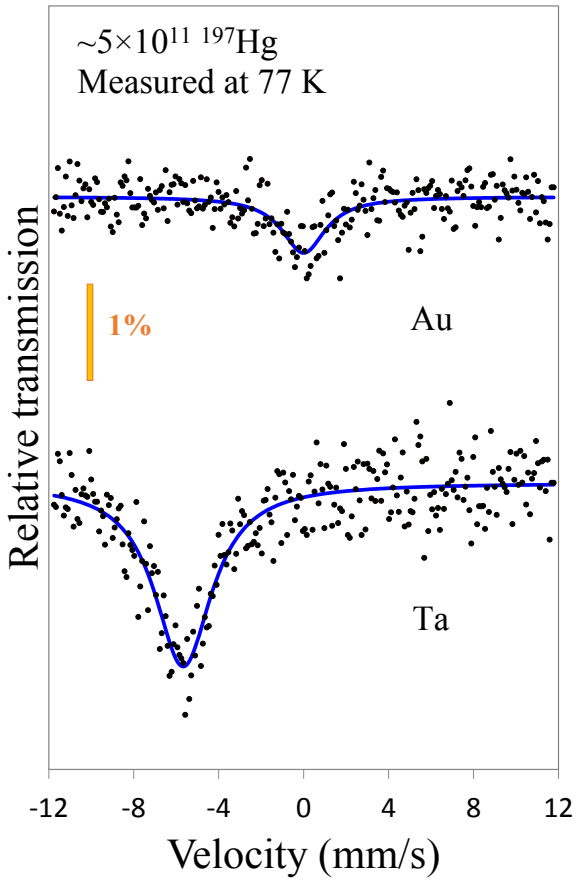

Fig. 3: 197Au emission Mössbauer spectra obtained with the source (197Hg in Au and Ta metals) and absorber (Au foil) at 77 K.

[1] H. P. Gunnlaugsson, New emission Mössbauer spectroscopy studies at ISOLDE in 2015, talk given at the Isolde workshop 2015, http://indico.cern.ch/event/437713/session/11/contribution/45
[2] http://indico.cern.ch/event/464984/
[3] http://iks32.fys.kuleuven.be/indico/event/31/

Local distortions in Sm orthochromite

Results of experiment IS487

Gonçalo Oliveira

Rare-earth orthochromites of the formula RCrO3 R=Dy, Pr, Ho, Yb, Er, Y, Lu, Sm are currently at the center of great controversy regarding ferroelectricity. While dielectric constant anomalies near 400-500 K in the heavier rare-earth chromites were associated with non-centrosymmetry other claim that the polarization observed

in these systems is due to the combined effect of the electric applied field that breaks the symmetry and the exchange-field on the R ion from the Cr sub-lattice. Accordingly, no spontaneous ferroelectric polar-order exists in these systems and the presence of a magnetic R-ion is essential to induce a metastable ferroelectric state. Contrarily, the appearance of ferroelectricity without any correlation to the magnetic order, arising from polar octahedral rotations and/or cation displacements, was recently claimed [1,2].

Clearly, additional efforts are needed to definitely validate these claims. Since these properties might emerge from local structural landscapes that are not well described by long-range average structural methods, the use of local probe studies, such as Perturbed Angular Correlation (PAC) spectroscopy, provide relevant knowledge.

In this work $SmCrO_3$ compound was studied. The temperature dependent of the electric field gradient (EFG) on $SmCrO_3$ compound was followed, using the ^{111}Cd PAC probe, in the 16 K<T<723 K temperature range (see Fig. 1). A temperature range that spans over the important transition temperatures, namely the reported ferroelectric transition (T_{FE}≈220 K), the magnetic ordering of Cr atoms sub-lattice (T_N^{Cr}=133 K), the spin reorientation (T_{SR}=34 K) and magnetic ordering of Sm atoms sub-lattice (T_N^{Sm}=20 K). The ^{111m}Cd implantation and ^{111}Cd->^{111}In diffusion was followed by an annealing at high temperatures in air.

At high temperatures, T>300 K, a frequency triplet corresponding to a single EFG, *i.e.*, one probe local environment, was observed and in this temperature range no significant changes occur in the spectra when the temperature is lowered. However, below 300 K visible changes can be observed in the perturbation function (R(t)) data and in the corresponding Fourier transforms. In detail, a second EFG emerges and its relative abundance increases with decreasing temperature. Accordingly, the fits to the R(t) experimental data were performed considering only one static EFG distribution, which was assumed to be Lorentzian-like, for T>300 K while two EFG distributions had to be considered to account for the features that emerge below that temperature.

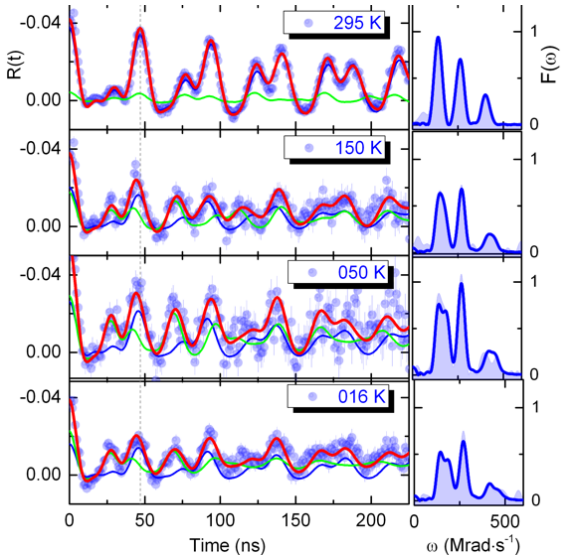

Fig. 1: Representative R(t) functions, corresponding fits and respective Fourier transform at different temperatures for $SmCrO_3$.

The spectra obtained at high temperatures revealed an EFG characterized by a V_{ZZ}^{Sm1}≈76 V/m^2 and an asymmetry parameter η≈0.2 in good agreement with similar systems. The second EFG, that emerges at low temperatures, is characterized by a similar fundamental frequency but a higher asymmetry parameter η≈0.6.

From our data we observed that a distortion of the high temperature local environment start to develop below 300 K within the paramagnetic phase. Although our data might be compatible with the most recent reports, where polar octahedral rotations and/or cation displacements are at the origin of a polar order in the paramagnetic state, remarkably, our results point to a more subtle scenario, where locally an inhomogeneous state emerges. In this new state regular and distorted environments (most probably polar and non polar states) coexist.

[1] http://doi.org/10.1103/PhysRevB.86.214409.
[2] http://10.1209/0295-5075/107/47012.

Post Data Processing of ^{111m}Cd-PAC Measurements on $LiNbO_3$

Results of experiment IS492
Website: http://ssp.web.cern.ch/ssp/info.htm

Jens Röder
(for the Solid State Physics collaboration)

The development of digital perturbed angular correlation (PAC) [1,2], permits the digital storage of an entire PAC measurement as time and energy values for each detected event. As a result, post analysis allows additional scientific results to be explored, beyond the reach of traditional PAC where the selection of distinct energy windows reduces the amount of collected data.

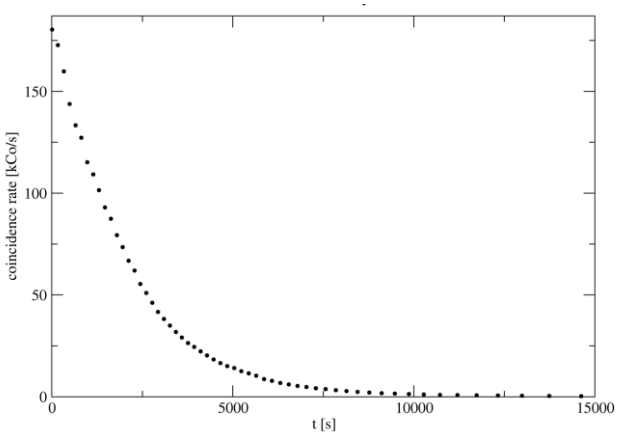

Fig. 1: Coincidence rate vs time from digital spectrometer of ^{111m}Cd PAC on $LiNbO_3$

Here, the advantages of post processing PAC data are shown. In the following example a single crystal of $LiNbO_3$ was implanted with ^{111m}Cd and annealed at 800°C. The PAC measurement was performed at room temperature and total No of 2.26E9 γ-quants were collected. This yielded a total No. of 2.4E8 coincidences (Co). The sample had a high activity of 6.6 MBq at the beginning of the measurement and therefore a top coincidence rate of 180 kCo/s was observed, see Figure 1. Due to the short half-life of ^{111m}Cd, with 48.5 minutes the coincidence rate decreases rapidly to 100 Co/s in 5.3 h. As a property of resistor voltage dividers in photocopiers for the dynodes, we observed a shift of the γ-energies in the channels at high activities. The energy peak shifts, as seen in Figure 2 in the green energy spectrum, have been corrected by separating the 70,647 data sequences in sections of 10,000 providing each section with its own energy window settings. This prevents that the 171 keV energy peak of ^{111}In moves into the window setting of the 151 keV peak of ^{111m}Cd, which would result in a damping of the amplitude: ^{111}Cd anisotropy has inverted signs: positive for ^{111m}Cd decay and negative for ^{111}In decay but with identical numbers. Although the high count rate the FWHM of the 245.4 keV peak increased only by 54% and therefore provides still good energy resolution of the $LaBr_3$:Ce scintillator with 4.5% at 245 keV and 6.2% at 151 keV at these high count rates. At significantly lower count rates, the energy resolution reaches 1.6% for 245 keV and 2.6% at 151 keV which is significantly lower than proposed by the producer Saint Gobain who measured an energy resolution of 2.9% at 662 keV for a ^{137}Cs source.

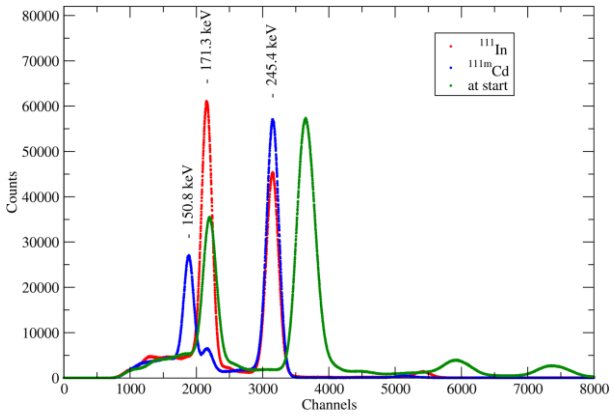

Fig. 2: Energy spectra of 111mCd and ^{111}In evolving over time including shifting to the left side.

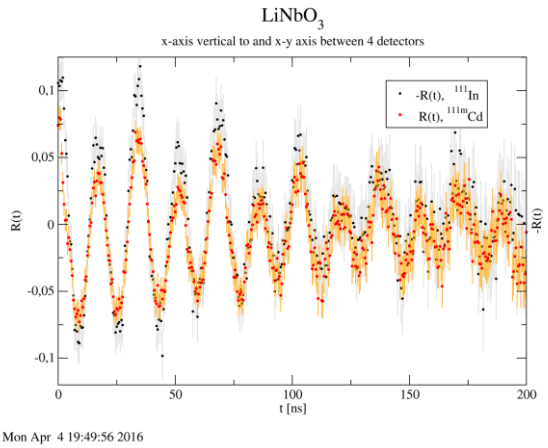

Fig. 3: Single crystal LiNbO3 annealed at 800°C for 30 min. ^{111m}Cd and ^{111}In as mother isotopes.

A thorough inspection of the data revealed the presence of 0.5% ^{111}In in the ^{111m}Cd beam steadily increasing by the end to 2.2%. Figure 2 shows the energy spectra at the beginning and the end of the measurement. The decay of ^{111m}Cd is seen in the blue spectrum with a significant higher peak for 245 keV γ-quants compared to 151 keV. At a later time in the red spectrum the decay of ^{111}In appears with a

lower peak for the 245 keV γ-quants compared to the 171 keV. Using time information in the data the count rate could be obtained at different times of the measurement. The ^{111}In concentration could be corrected back to the time of implantation which sufficient to create an additional PAC spectrum from the already recorded data, showing the opposite anisotropies of ^{111}Cd from both ^{111m}Cd and ^{111}In decay. The PAC spectra should be identical when one of them is inverted. As shown in Figure 3 the amplitudes have a significant difference.

It has to be noted, that the conditions of implantation, annealing, sample position, and orientation between detectors were identical and therefore cannot contribute to this difference. Smaller energy windows had been applied to the data without a change in the amplitudes. The energy peak shifts induced by strong activity changes during the measurement, as seen in Figure 2, had been already corrected to prevent the 171 keV energy peak of ^{111}In moving into the window setting of the 151 keV peak of ^{111m}Cd. The difference may be a result of different annealing properties between In and Cd inside the $LiNbO_3$ crystal. The quadrupole interaction frequency ν_Q [3] of ^{111}Cd in $LiNbO_3$ could be obtained with a value of 194 MHz, with a broadening of 3 MHz, and η=0.1. In the Fourier transformed graph in the top of Figure 4, only two of the three expected transition frequencies for a 5/2 state are observed. This is due to the fact that when using 4 detectors in 90° the distribution of crystal axes is not uniform as for randomly orientated crystallites in powder samples and the direction of the EFG to the lattice coordinates becomes visible. In this measurement the y-axis of the crystal is vertical to the detector plane and the x-z axis angle bisector in direction to the detectors. As a result, the 3rd frequency is not present.

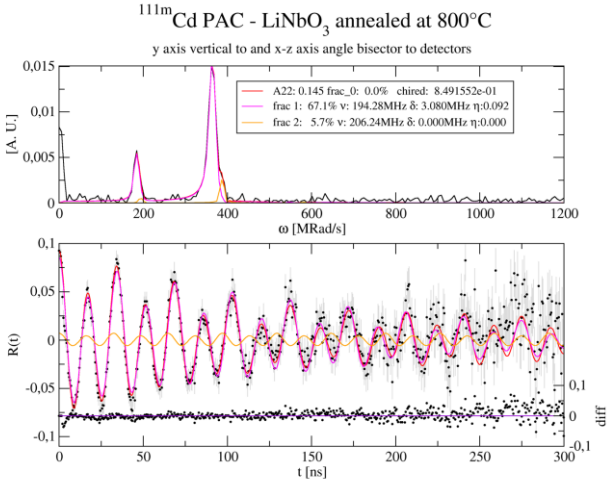

Fig. 4: Single crystal LiNbO3, fitted ^{111}Cd spectrum.

In Figure 5 the z-axis is vertical to the detector plane and the x-y axis angular bisectors in directions to the 4 detectors. Here only the 1st transition frequency is visible as shown in the Fourier graph. About 67% of the probes where in regular sites in Figure 4. A second frequency was observed with 206 MHz of about 6% of the probe atoms. This is in good agreement with the measurements of Hauer et al. [4]. The ^{111}Cd from ^{111}In decay revealed the same two frequencies but 87% of the Cd atoms where found on regular sites and about 6.6% contributed to the 206 MHz frequency. The difference of the fraction was to be expected from Figure 3. The $LiNbO_3$ of this measurement had a metal ratio of Li/Nb=0.995 and is a high purity material. The single crystals were cut in their axis directions and were polished. This sample was annealed in vacuum at 800°C for 30 minutes. A crystal with the metal ratio Li/Nb=0.94 and an annealing of 700°C in air for 30 minutes revealed a slightly higher quadrupole interaction frequency of 197 MHz with fraction of 58%, a broadening of 8 MHz and η=0, see Figure 5. Potentially there are 4 additional frequencies of low fraction of about 3% (ω =68, 80, 97, 127 MRad/s) that could yet not be identified but contribute to a frequency visible in the difference plot.

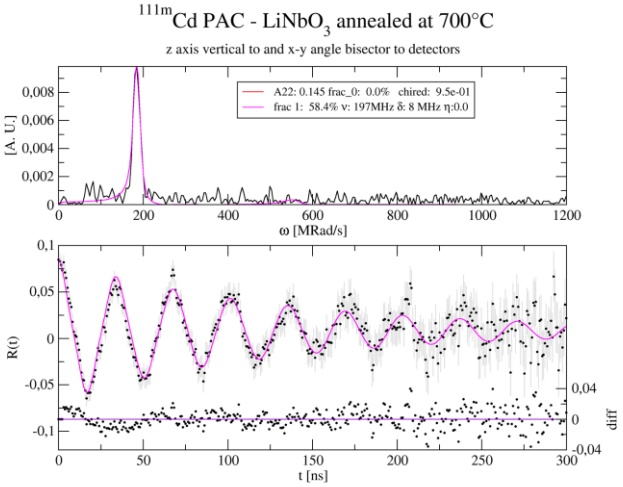

Fig. 5: Single crystal LiNbO3 Lithium depleted, fitted ^{111}Cd spectrum.

The motivation of the study of $LiNbO_3$ is to investigate the changes of the quadrupole interaction frequencies of samples of different purity. $LiNbO_3$ has a wide use in applications due to its properties. It is ferroelectric, nonlinear optic, electrooptic, photo-refractive, elastooptic, piezo-electric and pyroelectric. The ferroelectric Curie temperature is about 1143°C. Due to this high temperature applications e.g. actuators in Diesel engines are a common use. In THz generation by optical rectification $LiNbO_3$ crystals have been used [5]. Further it is

extensively used in the telecom markets [6], for laser frequency doubling [7], or charge gradient microscopy [8] and many more applications.

Conclusions

As a result from the post processing of data analysis, it is to be suggested to stop measurements with ^{111m}Cd beams sufficiently early after about 3 to 3.5 hours when using BaF_2 detectors with conventional machines to avoid an unwilling contribution of ^{111}Cd from ^{111}In decay. It is also proposed to make use of the ^{111}In in the samples that remains almost pure after 6 to 8 h at the implantation.

In $LiNbO_3$ a second frequency was found in almost stoichiometric high purity material. Lithium depleted material has a slightly higher ν_Q and potentially additional frequencies of low fraction.A continuation of the measurements is suggested to unfold the potential presents of the additional sites.

[1] C. Herden, J. Röder, J.A. Gardner, K.D. Becker. NIMA **594** (2008) 155-161
[2] J. Röder, c. Herden, J.A. Gardner, K.D. Becker, M. Uhrmacher, H. Hofsäss. Hypfine Interact. **181** (2008) 131-139
[3] R. Vianden. Hyperfine Interact. **4** (1978) 956
[4] B. Hauer, R. Vianden, J.G. Marques, N.P.Baradas, J.G. Correia, et al. Physical Review B **51** (1995) 6208-6214
[5] Y. Avestisyan, C. Zhang, et al. Opt. Exp. **20** (2012) 25753
[6] E.L Wooten, K.M. Kissa, A. Yi-Yan, et al. IEEE J. Sel. Top Quant. 6 (2000) 69-82
[7] J. Burghoff, C. Gribing, S. Nolte, A. Tünnemann. App. Phys. Lett. **89** (2006) 081108
[8] S. Hong, S. Tong, W.I. Park, Y. Hiranaga, Y. Cho, A. Roelofs. PANAS **111** (2014) 6566-6569

GEFÖRDERT VOM
Bundesministerium für Bildung und Forschung
ESF Europäischer Sozialfonds für Deutschland
Europäische Union
Zusammen. Zukunft. Gestalten.

Ground-state properties

Half-life and branching ratio of ^{37}K

Results of experiment IS527
Website:
http://www.cenbg.in2p3.fr/Superallowed-Fermi-transitions

Teresa Kurtukian-Nieto, B. Blank, Ph. Alfaurt, M. Aouadi, P. Ascher, G. Benzoni, A. de Roubin, M.Gerbaux, J. Giovinazzo, T.Goigoux, S.Grévy, J. Grinyer, M. Kowalska, M. Madurga, C.Magron, A.I. Morales and J.-C. Thomas

Nuclear β decay is an excellent probe to study the properties of the atomic nucleus. As β decay is governed by the weak interaction, it may also be used to test the light-quark sector of the Standard Model (SM). The comparative half-life *ft* of $0^+ \rightarrow 0^+$ β-decaying nuclides gives access to the vector coupling constant g_v which together with the muonic vector coupling constant allows for the determination of the up-quark down-quark element V_{ud} of the Cabibbo-Kobayashi-Maskawa quark-mixing matrix, which, according to the SM, is unitary [1].

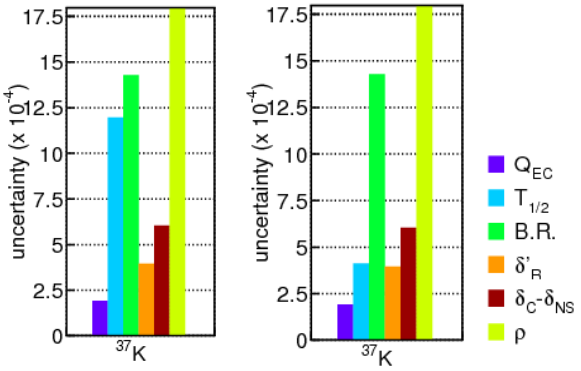

Fig. 1: The figure summarizes the uncertainties associated with the different parameters used to determine the corrected Ft value in the case of ^{37}K before (left) and after (right) the present experiment. As can be seen, the uncertainty on the half-live has been significantly reduced.

In this work, we present a study of the half-life and the branching ratio of $^{37}_{19}K_{18}$, which decays to the mirror nucleus $^{37}_{18}Ar_{19}$. The experimental quantities necessary for the determination of ft are: the β-decay energy Q_{EC}, the half-life $T_{1/2}$, and the super-allowed branching ratio BR. The theoretical corrections δ_C, δ_{NS} and δ'_R must be determined by models [2]. However, for the decay between mirror nuclei, the Gamow-Teller β decay contributes to the decay strength for the isobaric analog state in the daughter nucleus, and the Gamow-Teller to Fermi ratio ρ [3,4] must be measured. As can be seen from Figure 1, $T_{1/2}$ and BR were the second and third most important contributors to the overall precision, with ρ having the most important contribution to the error.

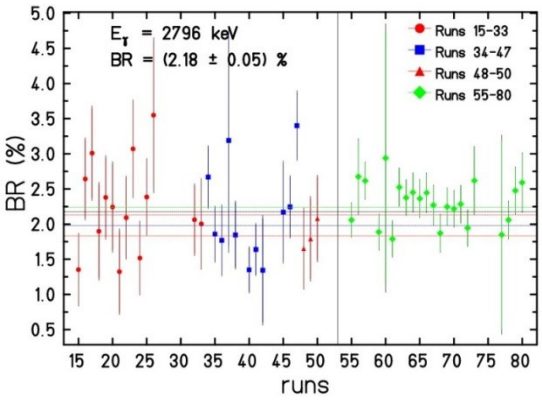

Fig. 2: Branching ratio as a function of the run number. Different symbols correspond to different experimental conditions.

The ^{37}K isotopes were produced by spallation reactions in a CaO target, induced by the PS Booster proton beam. Mass A=37 nuclei were selected by the GPS and sent to the LA1 beam line of ISOLDE. At LA1, the beam was intercepted by an aluminized Mylar tape. After the accumulation, the tape transported the activity to a plastic scintillator and a precisely efficiency calibrated germanium detector [5]. At this detection position, the activity decayed for a given time before the residual activity was evacuated towards the tape storage shielded from the detectors. For the half-live different possible biases of the results were searched for, due to experimental parameters like detector high voltage or threshold as well as dependences of the results on analysis parameters. The present result $(1236.37 \pm 0.28_{stat} \pm 0.46_{sys})$ ms has a precision of 0.04% and is in agreement with the recent experimental result from Texas A&M [6].

Our result for the branching ratio of the 2796 keV γ ray is (2.18 ± 0.17) %, yielding a precision of the super-allowed transition of 0.17 %. The precision for the intensity of the 2796 keV γ ray is of only 8 % which is largely due to a pile-

up problem. The statistical uncertainty is about a factor of three smaller as can be seen in Figure 2. Therefore, a precision of 2% on the intensity of the 2796 keV γ ray - yielding at the end a precision of ~4 x10^{-4} on the super-allowed transition- should be obtained with a better treatment of the pile-up in a future experiment.

[1] J.C. Hardy, I.S. Towner, Phys.Rev.C**91** 025501 (2015)
[2] I.S. Towner, J.C.Hardy, Phys.Rev.C**77** 025501 (2008)
[3] N. Severijns, et al., Phys. Rev. C **78**, 055501 (2008)
[4] O. Naviliat-Cuncic, N. Severijns, Phys. Rev. Lett. **102**, 142302 (2009)
[5] B. Blank et al., Nucl. Instrum. Meth. A **776**, 34 (2014)
[6] D. Shidling et al., Phys. Rev. C 90, 032501 (2014)

Mass measurements and α-decay spectroscopy combine for polonium with ISOLTRAP

Results of experiment IS513
Website: http://isoltrap.web.cern.ch

Numa A. Althubiti
(for the ISOLTRAP collaboration)

A special feature of the neutron-deficient lead region is the degeneracy between the 3/2$^-$ and 13/2$^+$ energy levels in even-Z, odd-N isotopes, typically associated with the $\nu p3/2$ and $\nu i13/2$ orbitals, as well as isomeric 10$^-$ states in the odd-Z, odd-N isotopes [1,2]. Previous studies in this region, using ISOLTRAP in combination with in-source laser purification [3] and decay spectroscopy [2,4] have already contributed in tracking the excitation energy across a long chain of isotopes. There remains, however, a gap in the knowledge where the two states are closest in energy, and the question of whether the 13/2$^+$ ever becomes the ground state. To resolve these issues, we proposed to measure the excitation energy of these states in ^{195}Po and ^{197}Po.

Instead of placing the decay setup behind the precision Penning trap as earlier for Tl [2], we employed ISOLTRAP's multi-reflection time-of-flight mass spectrometer (MR-TOF MS) [5]. Most Po contaminations are surface-ionized Tl isobars, which are easily removed by the MR-TOF MS. Therefore, the new CRIS decay-spectroscopy station (DSS2.0) [6] was installed directly downstream.

The resonant ionization laser ion source (RILIS) was used to selectively enhance either the isomer or the ground state [7,8]. An MR-TOF-purified beam of Po was then delivered to either the DSS2.0 or the Penning traps. The α-decay spectroscopy supported the mass measurements by providing an accurate measurement of the ground-state-to-isomer count ratio for a given RILIS frequency setting. The decay measurements were used to identify the ions from the recorded α-decay energies by two Si detectors mounted inside the chamber on both sides of a thin carbon foil (90 nm). In addition, the decay chamber was surrounded by three germanium detectors (Ge1, Ge2, Ge3) for α-γ coincidence measurements, as can be seen in Fig. 1.

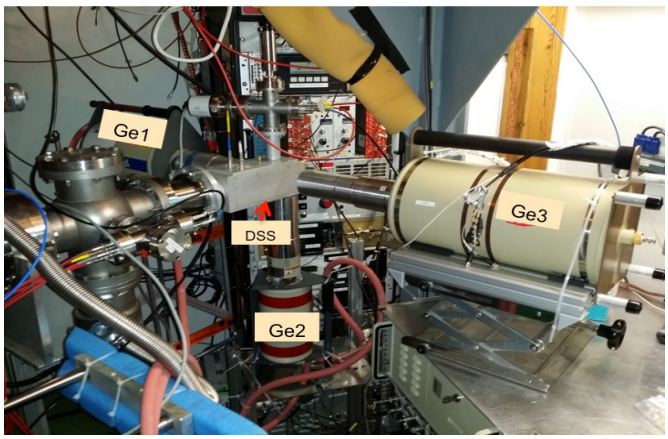

Fig. 1: The DSS2.0 setup. Three coaxial, high-purity germanium detectors surround the setup to offer an efficiency of 0.66% at 1 MeV.

Following the measurements of the α-decay energies, the masses of ^{195}Po and ^{197}Po were determined with relative uncertainties of the order of 10^{-8} using the precision Penning trap.

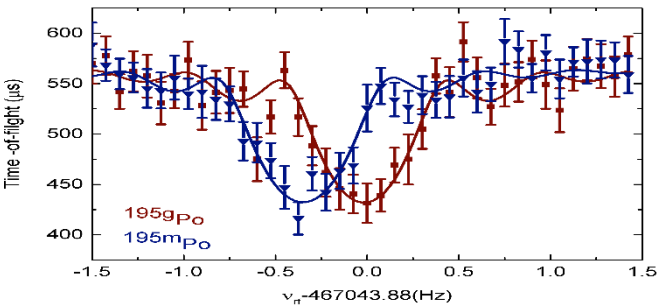

Fig. 2: Time-of-flight spectrum of ^{195}Po, the two states obtained from two different laser frequency settings with RILIS.

The complex hyperfine structures of the odd-A Po isotopes only allow the production of a pure high-spin state, while the low-spin state always comes as part of a mixture [8,9].

However, in addition to the RILIS selectivity, the half-life difference of the two ^{195}Po states allows modification of the ratio between them by storing the ions in the preparation trap, thereby enhancing the presence of the longer-lived, low-spin state.

By use of the extracted mass values of $^{195,197(g,m)}$Po, the excitation energies of the 13/2$^+$ state were measured in these isotopes for the first time, from which the excitation energies of similar states linked by α-decay chains was also determined. Furthermore, the ordering between the 13/2$^+$ and 3/2$^-$ states was determined for the first time. New decay spectroscopy data collected in isobar-free conditions are still under analysis.

[1] C. Van Beveren, et al., Phys. Rev. C **92**, 014325 (2015).
[2] J. Stanja, et al., Phys. Rev. C **88**, 054304 (2013).
[3] C. Weber, et al., Phys. Lett. A **347**, 81-87 (2005).
[4] Ch. Böhm, Ch. Borgmann, et al., Phys. Rev. C **90**, 044307 (2014).
[5] R.N. Wolf et al., Int. J. Mass. Spectrum. 349-350, 123-133 (2013).
[6] K. M. Lynch, T.E. Cocolios, N. A. Althubiti, G. J. Farooq-smith, A. J.Smith, Nucl. Inst. And Meth. A, in preparation.
[7] T.E. Cocolios, B.A. Marsh, et al., Nucl. Instrum. Meth. B **266**, 4403-4406 (2008).
[8] T. E. Cocolios et al., J. Phys. G **37**, 125103 (2010).
[9] M.D. Seliverstov, T.E. Cocolios, et al., Phys. Lett. B **719**, 362-366 (2013).

Mass spectrometry of neutron-rich copper isotopes: a view of ^{78}Ni from only one proton away

Results of experiment IS535
Website: http://isoltrap.web.cern.ch

André Welker
(for the ISOLTRAP collaboration)

Based on its proton and neutron numbers (28 and 50, respectively) ^{78}Ni is supposed to be a doubly magic nuclide. However, experimental evidence is scarce. Only recently, hints of double magicity were given by a measurement of β–decay half-lives at RIKEN [1]. While the direct study of the properties of ^{78}Ni is still very difficult (impossible at ISOLDE), a common approach is to study indirectly the strength of the Z = 28 and N = 50 cores in neighboring nuclides. Having only one additional proton, ^{79}Cu makes an excellent indirect probe.

The experiment was conducted using ISOLTRAP [2] in July, 2015. Copper isotopes were produced by fission processes in the UC_x-target, induced by neutrons from a spallation converter and selectively ionized using RILIS. This experiment extended several previous studies of mass spectrometry [3], collinear laser spectroscopy [4] and in-source laser spectroscopy [5]. The mass measurements of $^{77-79}$Cu were performed with ISOLTRAP's multi-reflection time-of-flight mass spectrometer (MR-ToF MS) [6]. The main (surface-ionized) isobaric contaminants Rb and Ga were identified in the Penning trap and then used as calibration ions during the MR-ToF determination of the copper-isotope masses. The release of ^{77}Cu from the target exceeded 250 ions/proton pulse (pp), compared to the yield of ^{78}Cu with 31 ions/pp and for ^{79}Cu with 7 ions/pp.

The MR-ToF spectrum of A=79 is shown in Figure 1.

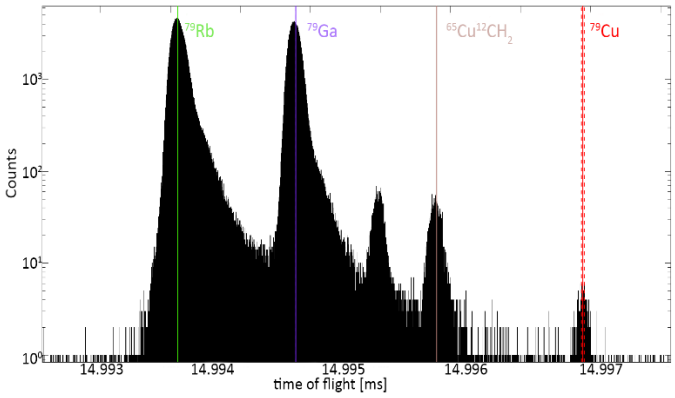

Fig. 1: MR-ToF spectrum showing ^{79}Cu, the abundant isobaric contaminants ^{79}Rb and ^{79}Ga plus a molecule, identified as $^{65}Cu^{12}C^{1}H_2$.

The yields of $^{77-78}$Cu made it feasible to also measure their masses with the precision Penning trap, with the MR-ToF used to cleanly separate the copper isotopes. Figure 2 shows the time-of-flight ion cyclotron resonance of ^{78}Cu.

The isomer in ^{76}Cu, which was proposed following a beta-decay measurement [8], was not seen by ISOLTRAP, neither earlier [3] nor during the 2015 run. We also used trapped-ion transmutation [9] by beta decay of ^{75}Cu to ^{75}Zn. The recoiling daughter nuclide was held in the buffer-gas-filled preparation Penning-trap and transported to the

precision Penning-trap for the mass measurement. Two ^{75}Zn isomers were discovered.

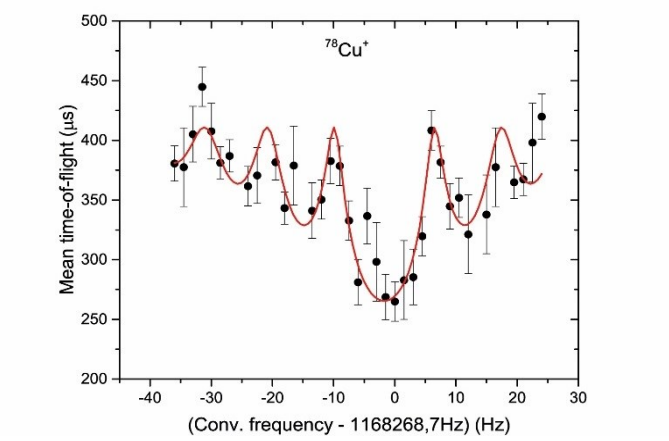

Fig. 2: Time-of-fight ion cyclotron resonance of ^{78}Cu obtained with a quadrupole excitation time of 100 ms. The solid (red) line shows the fit of the expected resonance curve to the data [7].

Combining the new mass values with shell-model calculations is expected to enhance the understanding of the observed inversion of the levels in ^{75}Cu [4] and will allow us to explore the trend of ground-state binding energies up to *N*=50.

[1] Z. Y. Xu *et al.*, Phys. Rev. Lett.. **113**, 032505 (2014).
[2] S. Kreim *et al.* Nucl. Instrum. Methods Phys. Res., Sect. B **317**, 492 (2013).
[3] C. Guénaut *et al.*, Phys. Rev. C, **75**, 044303 (2007).
[4] K. T. Flanagan *et al.*, Phys. Rev. Lett. **103**, 142501 (2009).
[5] U. Koester *et al.*, Phys. Rev. C **84**, 954 (2011).
[6] R.N. Wolf et al. Int. J. Mass Spectrom. **349-350**, 123–133 (2013).
[7] M. König *et al.* Int. J. Mass Spectrom Ion. P. **142**, 95 (1995).
[8] J. A. Winger *et al.*, Phys. Rev. C **42**, 954 (1990).
[9] A. Herlert et al., The Eur. P. J. A, **48**, 97 (2012).

2015 at the Collinear Resonance Ionization Spectroscopy experiment

Results of experiment IS471, IS531, IS571
Website: http://isolde-cris.web.cern.ch/isolde-cris/

Shane Wilkins
(for the CRIS collaboration)

The Collinear Resonance Ionization Spectroscopy (CRIS) programme on francium isotopes was started at ISOLDE in 2011. At the end of 2014, the first high-resolution experiment was performed allowing quadrupole moments to be determined. Two papers from this experiment have been published this year [1,2], with a third in preparation [3]. An overview of the high-resolution technique is presented with the quadrupole moment of ^{219}Fr in [1] and the results of combined laser and decay spectroscopy of low-lying states in ^{206}Fr, ^{202}At, ^{198}Bi are presented in [2].

In 2015, the high-resolution CRIS technique was extended to two new elements: copper and gallium. This was made possible by the installation of two new high-resolution continuous-wave lasers in the new CRIS laser laboratory located in Building 508. A Matisse dye laser produced light for the copper experiment and an M-Squared SolsTiS titanium-sapphire (Ti:Sa) laser produced light for the gallium and francium experiments. The first three-step high-resolution resonance ionization scheme was executed successfully to study gallium allowing measurements up to ^{82}Ga. The realization of three-step schemes increases the number of elements CRIS is able to study as most require three or more steps to resonantly ionize. The investigation into the neutron-deficient francium isotopes from previous campaigns at CRIS was extended further by measuring the quadrupole moment of ^{203}Fr for the first time. This represents the most exotic francium isotope measured in high-resolution to date.

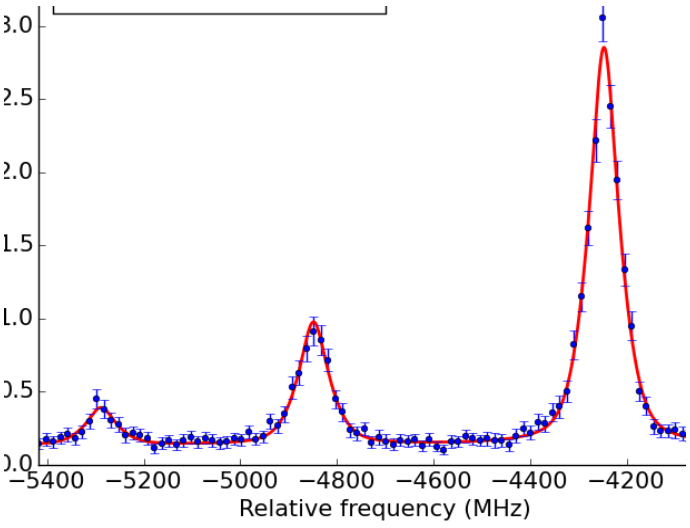

Fig. 1: Hyperfine spectrum obtained for ^{65}Cu using the 324 nm (high-resolution) + 266 nm (non-resonant) scheme resulting in a 70 MHz linewidth.

Two pulsed Ti:Sa cavities on loan from the University of Mainz have been installed alongside an injection-seeded system from Mainz/Jyväskylä, in which high-resolution light can be produced with photon densities of a pulsed system. The pulsed systems are all pumped by a new 10 kHz Nd:YAG Lee Laser purchased with an STFC (UK funding agency) grant. A frequency conversion unit has been constructed for use with the pulsed systems where up to fourth harmonic light can be produced. This will allow CRIS to access new wavelength regimes and develop ionization schemes for other atomic and ionic systems. Additionally, a new plasma ion source has been commissioned allowing the production of ion beams of a wide range of elements.

Ivan Budinčević successfully defended his thesis entitled 'Nuclear structure studies of rare francium isotopes using Collinear Resonance Ionization Spectroscopy (CRIS)' graduating with a Ph.D. from KU Leuven. The CRIS collaboration wishes him the best for the future. Kieran Flanagan's ERC grant entitled 'Fundamental nuclear properties measured with laser spectroscopy' started in April 2015 and through this, Ronald Fernando Garcia Ruiz joined the experiment as a postdoctoral research assistant with the University of Manchester.

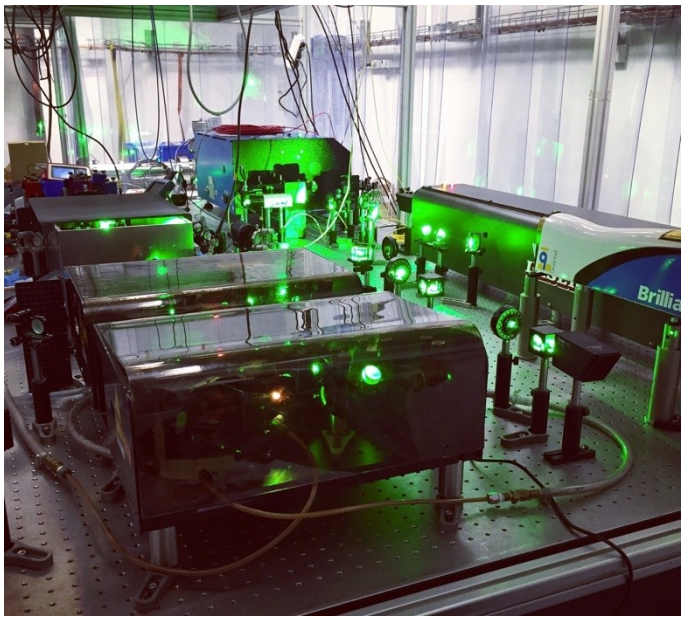

Fig. 2: The new Lee Laser pumping the pulsed Ti:Sa cavities and injection seeded system in the CRIS laser lab

[1] R. P. de Groote, I. Budinčević, et al., Phys. Rev. Lett. 115, 132501 (2015).
[2] K. M. Lynch, T. E. Cocolios, et al., Phys. Rev. C 93, 014319 (2016).
[3] G. J. Farooq-Smith, T. E. Cocolios, et al. (In preparation).
[4] I. Budinčević, CERN-THESIS-2015-236 (2015).

Test of Many-Body QED by Laser Spectroscopy of Short-Lived Isotopes

Results of experiment IS449

Wilfried Nörtershäuser
(for the COLLAPS collaboration)

Measurements of the absolute transition frequencies in the Be^+ $4s\ ^2S_{1/2} \rightarrow 4p\ ^2P_{1/2}$ and the $4s\ ^2S_{1/2} \rightarrow 4p\ ^2P_{3/2}$ fine-structure transitions of various beryllium isotopes were used to validate latest calculations in nonrelativistic quantum-electrodynamics (QED) [1]. Fine-structure splittings in helium and helium-like ions have attracted much interest as a test of bound-state QED for a long time. Theory was previously restricted to two-electron systems that were on the edge of feasibility concerning highly accurate calculations of this observable. This has recently been extended to three electrons and calculations were carried out for the resonance lines of atomic lithium [2] and of singly charged beryllium ions. An improvement of about two orders of magnitude was achieved compared to the best previous calculations and exceeded experimental accuracy by more than one order of magnitude. The only stable isotope ^{9}Be unfortunately exhibits unresolved hyperfine structure in the $4s\ ^2S_{1/2} \rightarrow 4p\ ^2P_{3/2}$ transition, which complicates the extraction of the fine structure splitting. The same is true for all odd isotopes in this chain. However, at ISOLDE we had access to the unstable even-even isotopes ^{10,12}Be that have no nuclear spin and therefore no hyperfine splitting, strongly facilitating the extraction of the fine structure splitting.

In the experiment, performed already in 2011, the absolute transition frequencies of $^{7,9\text{-}12}$Be were measured with a frequency comb. This device allows to directly transfer the accuracy of a microwave clock (in our case a Rb clock) into the optical regime by precisely controlling the repetition rate and the so-called carrier-envelope offset of a femtosecond laser. Recording a beat note with the continuous wave laser used for the spectroscopy allowed us to determine the transition frequencies with accuracy of

better than 1 MHz, representing a relative precision of better than 10^{-9}. Uncertainty from the insufficiently known starting potential of the ions inside the ISOLDE ion source was eliminated by performing collinear and anticollinear measurements quasi-simultaneously, rapidly switching the laser beams in the two directions while integrating the fluorescence signal.

We have previously determined and published the isotope shifts in order to extract the nuclear charge radii of $^{7,9-12}$Be including the one-neutron halo nucleus ^{11}Be [3,4]. Evaluating now the absolute transition frequencies we first found good agreement with the calculated splitting isotope shifts (SIS), i.e., the isotope dependent differences in the fine-structure splitting as is shown in the left of Fig. 1. The red dots represent the theoretical values that have uncertainties much smaller than the symbols, while blue and green symbols represent the experimental results. We then used the calculated shifts to combine the fine structure splitting information obtained along the complete isotopic chain to improve the experimental value of the fine-structure splitting of the stable isotope ^{9}Be as shown in the right part of Fig. 1. The obtained value has an uncertainty reduced by more than two orders of magnitude compared to the most accurate previous measurement and is in reasonable agreement with the theoretical prediction.

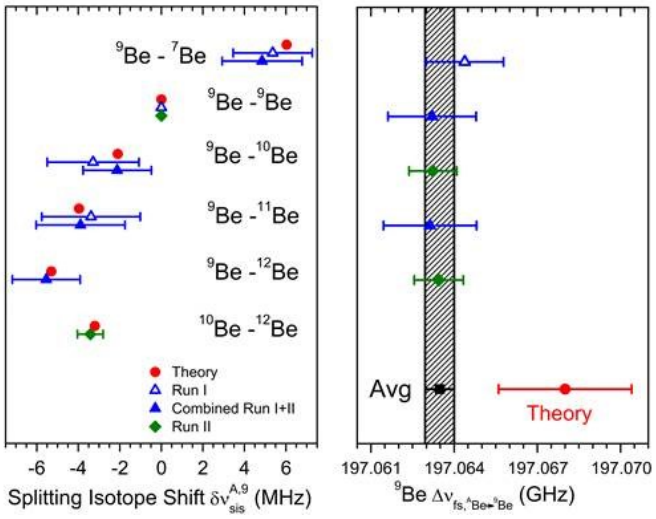

Fig. 1: Experimental results and comparison with theory for the splitting isotope shift SIS relative to ^{9}Be (left) and for the fine structure splitting of all isotopes transferred to ^{9}Be (right). The legend belongs to both graphs [1].

[1] W. Nörtershäuser et al., Phys. Rev. Lett. **115**, 033002 (2015).
[2] M. Puchalski and K. Pachucki, Phys. Rev. Lett. **113**, 073004 (2014).
[3] W. Nörtershäuser et al., Phys. Rev. Lett. **102**, 062503 (2009).
[4] A. Krieger et al., Phys. Rev. Lett. **108**, 142501 (2012).

First Use of Optical Pumping in ISCOOL to study Mn isotopes

Results of experiment IS508

Carla Babcock
(for the COLLAPS collaboration)

The technique of optical pumping in a cooler/buncher has been successfully applied for the first time at ISOLDE, in order to study the hyperfine structure of the odd-even isotopes $^{53-63}$Mn. Previous studies of atomic $^{51-63}$Mn, performed using collinear laser spectroscopy at the COLLAPS setup, have yielded the magnetic dipole moments of these isotopes (Ref. [1,2]), however the quadrupole splitting of the atomic ground state transitions was too small to allow the extraction of the electric quadrupole moments.

Comparisons of the magnetic moments with shell model calculations have shown that neutron excitations across N = 40 are necessary to describe the properties of neutron rich Mn isotopes (Ref. [1,2]). As these excitations are associated with a strong onset of deformation, quadrupole moments provide complementary information on the ground state structure of the Mn isotopes.

In order to probe the quadrupole moments, it was necessary to perform spectroscopy using a transition with greater sensitivity to the quadrupole interaction. Such a transition was known in ionic manganese (Ref. [3]), from a metastable state, however the natural population of the metastable state is too low for efficient spectroscopy. The population of this state was therefore enhanced using optical pumping, a technique in which a laser beam is overlapped with the ions to excite them to an intermediate unstable state, from which they decay into the metastable state.

In order to increase the efficiency of the naturally weak optical pumping transition, it was necessary to have a long laser-ion interaction time. This was accomplished by

performing the optical pumping in ISCOOL, ISOLDE's cooler/buncher, where the ions are normally trapped for tens or hundreds of milliseconds before being released to the COLLAPS experiment as a bunch. This trapping time provides a good opportunity for multiple laser-ion interactions, while the laser linewidth is well matched to the Doppler-broadened profile of the ions. ISCOOL was realigned in order to create a direct path through its multiple apertures to allow laser entry into the bunching region (Fig. 1). Once a line of sight was established, an extra laser was diverted from the RILIS cabin, passing through one HRS magnet and entering ISCOOL through the injection side.

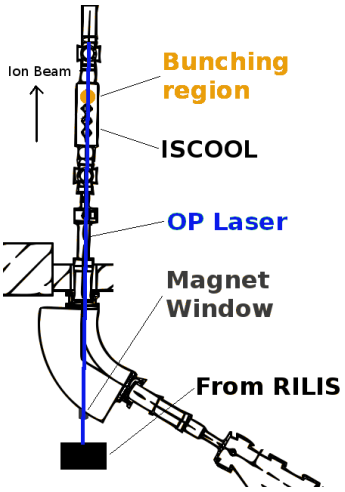

Fig. 1: Laser entry path for the optical pumping laser into the bunching region of ISCOOL.

The population of the metastable state was significantly enhanced through the use of optical pumping, as shown in Fig. 2. Spectroscopy was then performed from this level, yielding the quadrupole moments for the odd-even isotopes $^{53\text{-}63}$Mn. The results of this experiment have also allowed the mean-square charge radii of the isotopes to be extracted using two independent transitions to aid calibration.

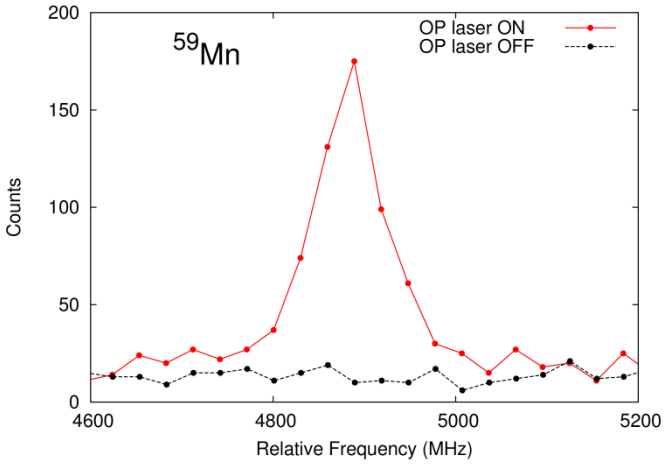

Fig. 2: Counts with optical pumping laser on compared to counts with laser off.

[1] C. Babcock et. al., Phys. Lett. B, 750:176-180, 2015.
[2] H. Heylen et. al., Phys. Rev. C, 92:044311, 2015.
[3] F. Charlwood et al., Phys. Lett. B, 690:346-351, 2010.

Beta-decay studies

Spectroscopy of $^{148-150}$Ba via β decay

Results of experiment IS579

Giovanna Benzoni, Razvan Lica
(for the IS579 collaboration)

Most nuclei are deformed, the prolate and oblate shapes being the most common ones due to the dominance of quadrupole degrees of freedom. In some specific cases higher order of multipolarity are expected.

Ba isotopes are located in a region of the Segrè chart characterized by a variety of shape phenomena, including shape coexistence and possible static octupole deformations. Higher order deformations can have a strong influence on γ-decay rates and on quasi-particle energies of the nuclei, which are, in turn, inputs for the various theoretical models developed to describe nuclei in this region [1, 2].

In the Ba isotopic chain alternating-parity bands, with large and constant B(E1) transition moments, have been found in $^{140-144}$Ba; the neighboring nucleus, ^{146}Ba, shows instead slower E1 transition rates than ^{144}Ba. The behavior of the alternating-parity states in ^{148}Ba in fact resembles the situation of ^{144}Ba more than that of ^{146}Ba, with no sign of back bending at increasing values of the angular momentum [3].

Access to the most exotic isotopes in this chain has been difficult so far: they are populated as fission fragments both in natural and induced fission, but, since no low-lying states are known, it is very difficult to pin them down.

These arguments have been at the basis of the experiment IS579 which aims at populating the Ba chain up to mass A=152 by means of the β decay of Cs isotopes. Ba isotopes ranging from A=148 to A=150 have been produced at ISOLDE using a micro-structured UCx target. The intensity of the A=150 beam was in the order of 2 Ions/μC, thus preventing any studies of the more exotic isotopes.

The experiment was performed using the Isolde Decay Station (IDS), equipped with 3 plastic scintillators to detect the β particles, 4 Clover detectors for the detection of γ rays following the decay of the daughter nuclei, and 3 small-volume $LaBr_3$:Ce detectors to perform Fast-Timing measurements and extract information on the lifetime of specific nuclear states. A picture of the setup is shown in Fig.1.

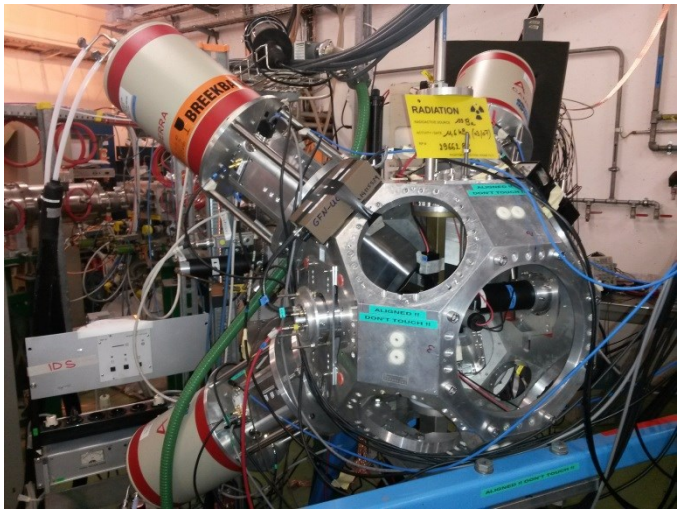

Fig. 1: IDS setup used during the IS579 experiment. The Clover detectors are visible on the left part of the figure, while $LaBr_3$:Ce and one of the plastic scintillators are located inside the support.

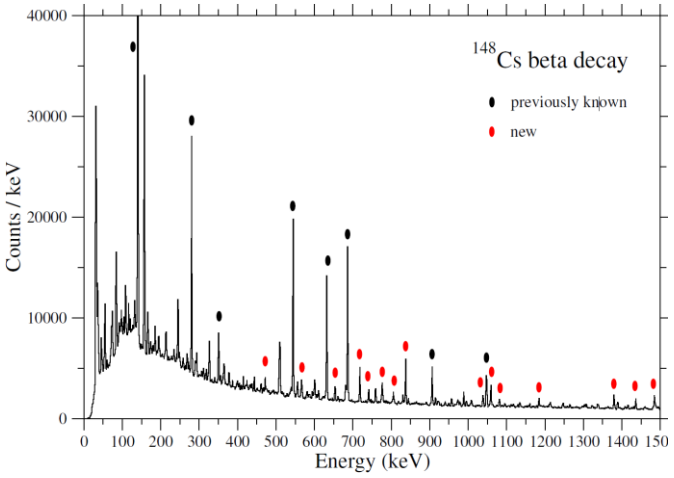

Fig. 2: Transitions measured in coincidence with the decay of ^{148}Cs in a time window of 350 ms after the proton pulse. Transitions belonging to the decay of ^{148}Ba are indicated: black dots show previously established transitions, while new ones are marked with red dots.

The half-lives for the decays ^{148}Cs->^{148}Ba, ^{149}Cs->^{149}Ba

and ^{150}Cs->^{150}Ba could be extracted from the analysis, resulting in 152±2 ms, 83±3 ms and 67±3 ms, respectively. Measured β-delayed neutron emission probabilities range from 35% in ^{148}Ba to 45% in the most exotic isotope.

The high statistics collected for the internal decay of ^{148}Ba allowed to perform γ–γ correlations therefore extending the existing level scheme up to 2.5 MeV. In Fig. 2, a spectrum showing transitions measured following the decay of ^{148}Cs is shown: known transitions are marked with black dots while newly established ones with red dots.

Transitions belonging to ^{149}Ba and ^{150}Ba have been studied for the first time, giving insight into the development of a stable deformation also in these isotopes.

The use of a Fast-Timing set up allows for the determination of B(E2) transition probabilities that will help in establishing the deformation parameter in the measured nuclei.

In the continuation of the experiment, expected to run in the coming summer, we plan to measure the decay from $^{150\text{-}152}$Cs.

[1] P.A. Butler and W.Nazarewicz, Rev. Mod. Phys. 68, 349 (1996).
[2] L.M. Robledo et al., Phys. Rev. C 81, 034315 (2010).
[3] W.Urban et al., Nucl. Phys. A 613, 107 (1997).

Beta-decay study of ^{20}Mg at IDS

Results of experiment IS507

Morten V. Lund
(for the IDS and MAGISOL collaborations)

The beta-decay of the dripline nucleus ^{20}Mg gives important information on resonances in ^{20}Na and ^{19}Ne, which are relevant for the astrophysical rp-process. In particular the spin and parity of the 2647-keV level in ^{20}Na and the partial width Γ_α of the 4033-keV level in ^{19}Ne are unsettled. Both quantities are important factors when determining the reaction rate of the breakout sequence of the HCNO cycle through the ^{15}O(α,γ)^{19}Ne(p,γ)^{20}Na reaction.

In order to settle these questions the IS507 experiment have studied the beta-decay of ^{20}Mg. The experiment was split in two parts in order to employ two different detector setups. The first experiment was performed in 2011 and was presented in the 2013 ISOLDE newsletter. The second experiment was performed in April 2015 at the IDS by using a compact geometry charged particle detection setup capable of particle identification in addition to the IDS HPGe-clover array. It was thus possible to measure charged particles and gamma rays as singles and as coincidences.

The beta-decay of ^{20}Mg has a 26.9(32)% [1] branching ratio for populating proton unbound resonances in ^{20}Na. Our measurement of the proton spectrum above 1.8-MeV can be seen on fig. 1. We observe the same features as seen in previous experiments [1,2], however, we do observe five additional proton peaks including beta-decay feeding to resonances above the Isobaric Analogue State (IAS) in ^{20}Na. Beta-delayed proton emission ends up in ^{19}Ne, which has two pairs of excited states with a spacing of roughly 30-keV. With the achieved energy resolution of the charged particle detectors it was not possible to distinguish proton branches to these different states in ^{19}Ne. Therefore, we used coincidences of protons and gamma rays in order to reconstruct the decay scheme and the intensities of the decay branches. The resulting decay scheme can be seen on fig. 2.

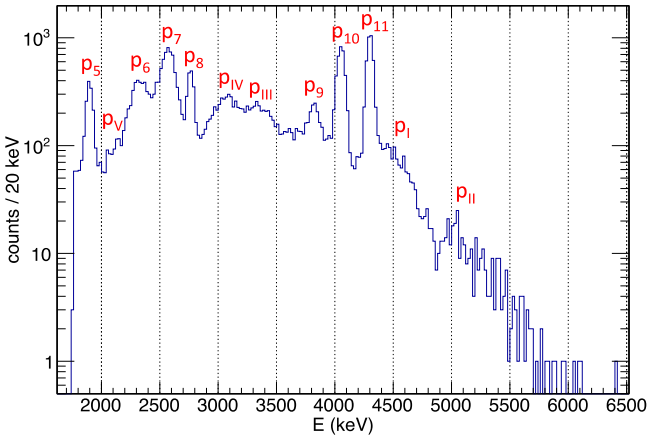

Fig. 1: Measured proton spectrum from the beta-decay of ^{20}Mg showing the center-of-mass energy.

Due to a large isobaric contamination of ^{20}Na, roughly a factor 8 more Na than Mg, we are not able to set a more stringent upper limit on the beta-decay feeding to the 2647-keV level than the existing upper limit of 0.2% [2].

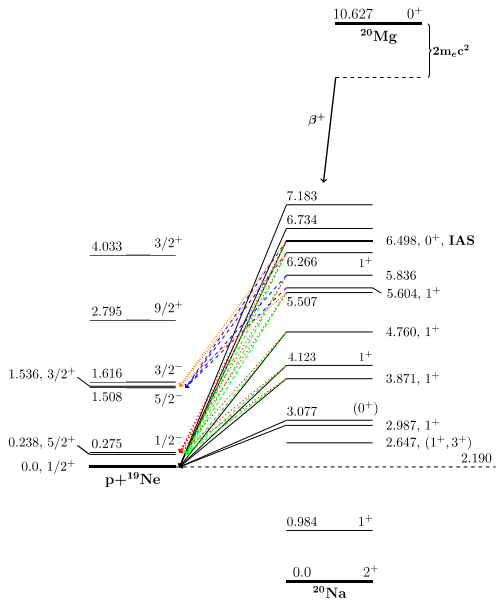

Fig. 2: Decay scheme for the beta-decay of ^{20}Mg.

However, for proton energies larger than 1.2-MeV we are able to produce clean proton spectra due to the use of a 20-μm thin silicon detector in the front of one of the charged particle telescopes. As a result we are able to observe three new proton unbound levels in ^{20}Na, to give much more accurate resonance energies for two levels, and to directly measure the beta-decay feeding to levels above the IAS (I_β = 0.66(2)%). The new information on levels above the IAS will be very useful in future studies of the 4033-keV level in ^{19}Ne.

The PhD thesis of Morten V. Lund, Aarhus University, is based on the results of the IS507 experiments.

[1] A. Piechaczek *et al.*, Nucl. Phys. A **584** (1995) 509.
[2] J.P. Wallace *et al.*, Phys. Lett. B **712** (2012) 59.

β decay of ^{6}He into the α + d continuum

Results of experiment IS505

Marek Pfützner and Karsten Riisager

The β decay of ^{6}He proceeds with a very small branching ratio (≈10^{-6}) to the final state of an α particle and a deuteron [1]. The probability of this β-delayed deuteron (βd) emission and the spectrum of emitted deuterons is sensitive to details of the initial wave function of ^{6}He, and thus offers a tool to probe its two-neutron halo structure (α+2n). The continuous βd spectrum of ^{6}He has been determined in the past, however, only for the decay energies larger than 400 keV in the α+d center of mass [2,3]. The reason for this threshold was pile-up and summing effects induced in silicon detectors by β-electrons emitted in the dominant decay channel of ^{6}He.

Knowledge of the low-energy part of the βd spectrum would help to constrain model parameters, and thus could shed light on the structure of the halo wave function of ^{6}He. Motivated by this challenge we applied a different detection technique employing the Optical Time Projection Chamber (OTPC) [4]. This detector allows to record tracks of charged particles, like ions, α-particles or deuterons, while remaining essentially insensitive to β-rays. The full 3D reconstruction of the tracks results from combination of the 2D image of the decay taken by a CCD camera with the drift-time profile measured by a photomultiplier. In the experiment, performed in August 2012, the ions of ^{6}He, were produced in a UC_x target, selected with the GPS separator, and subsequently bunched and accelerated to 3 MeV/u by the REX-Isolde facility. Finally they were implanted into the active volume of the OTPC filled with a gas mixture of 98% He + 2% N_2 at the atmospheric pressure. After implantation of each bunch, containing about 10^4 ions of ^{6}He, the CCD exposure and the drift-time profile recording were started for a period of 800 ms. During the total 106 hours of data taking about 2000 decay events of ^{6}He into an α particle and a deuteron were observed.

The reconstruction procedure was based on comparison of the total length of the track left by the α particle and the deuteron in the gas mixture, as well as the profile of energy-loss distribution along this track, with the simulations made with the SRIM2013 code [5]. It was found that this procedure yields reliable results for the decay energy down to 150 keV, corresponding to the deuteron energy of 100 keV. Finally, the data analysis resulted in 1651 well identified and reconstructed βd decay events of ^{6}He. For the absolute normalization of our spectrum we used the results of Raabe et al. [3], who achieved the most precise branching ratio for this decay channel.

The result is shown in Fig. 1. The integrated transition probability was found to be (2.39 ± 0.06 (stat) ± 0.15 (sys))

$\times 10^{-6}$ s^{-1} , which is about 70% larger than the intensity reported in Ref. [3]. The difference is made by the low-energy part of the spectrum, below the limit of the previous experiments.

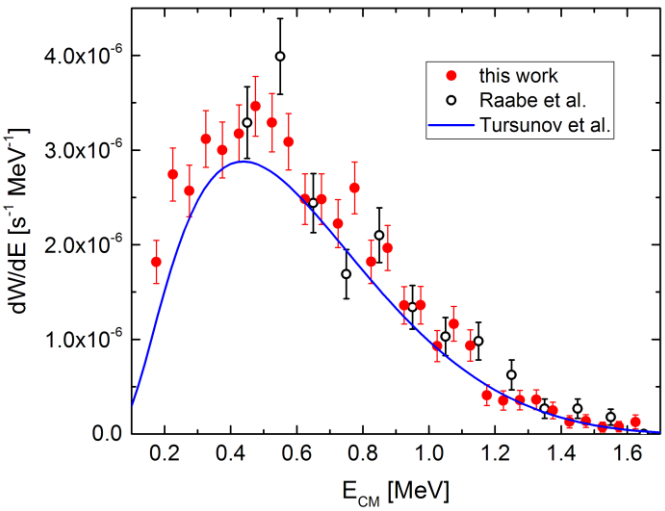

Fig. 1: Transition probability of the α + d branch in the β decay of ^{6}He as a function of the (α + d) energy. The results of this work are shown by the solid points while the open points are from Ref. [3]. The solid line represents the prediction from Ref. [6].

In Fig. 1 the prediction of the three-body model by Tursunov et al. [6] is also shown. While the shape of the predicted spectrum agrees well with the experiment, its intensity is about 20% too small. It remains to be seen if this discrepancy can be removed by tuning the α + d interaction alone, or improvements in the description of the ^{6}He halo wave function will be necessary.

The full account of the experiment and its final results are presented in Ref. [7].

[1] K. Riisager et al., Phys. Lett. B 235, 30 (1990).
[2] D. Anthony et al., Phys. Rev. C 65, 034310 (2002).
[3] R. Raabe et al, Phys. Rev. C 80, 054307 (2009).
[4] M. Pomorski et al., Phys. Rev. C 90, 014311 (2014).
[5] J.F. Ziegler, The Stopping and Range of Ions in Matter (SRIM), http://www.srim.org.
[6] E. M. Tursunov et al., Phys. Rev. C73, 014303 (2006).
[7] M. Pfützner et al., Phys. Rev. C92, 014316 (2015).

The exotic ^{11}Be(βp) decay

Results of experiment IS541

Karsten Riisager
(for the IS541 collaboration)

The recent observation at ISOLDE of the beta-delayed proton decay of ^{11}Be [1] was surprising in that the observed branching ratio of 8.3(9) 10^{-6} was more than two orders of magnitude above the best previous theoretical estimate [2] of 3.0 10^{-8}. Since the beamtime in this first experiment was limited, a second set of collections has been made in order to further cross-check for systematic errors. The results obtained so far are reported here.

In the experiment ^{11}Be is implanted in Cu samples, the intensity being monitored through observation of the 2125 keV line from the ^{11}Be decay in two sets of gamma-ray detectors: a standard Ge detector and LaBr detectors. The deduced collection rate of ^{11}Be per second is shown in the upper panel in figure 1 versus the mass setting of the HRS separator operating at 40 kV. The peak shape is partially due to the slit width used, the beam width was estimated to be less than 0.008 amu. The masses of ^{11}Be and ^{11}Li are 11.022 and 11.044 amu.

To further decrease the collected amount of ^{11}Li (whose decay also gives ^{10}Be) the beam gate was closed in the first 150 ms after proton impact on target. The halflives of ^{11}Li and ^{11}Be are 8.75 ms and 13.76 s. Samples were taken on the upper tail of the ^{10}Be peak to follow the separator lineshape over a larger dynamic range. Finally, samples were taken at the ^{11}Be mass position with the RILIS being blocked. This was done in order to test for the possible occurrence of ^{10}Be^{1}H ions. This important possible contaminant is not believed to survive through the ion source if produced in the target and would be reduced by dissociation by the RILIS laser beams, but only an indirect experimental limit on its production was possible in the earlier run and the present direct measurement is therefore essential.

The current set-up does not allow measuring the low-energy protons from the ^{11}Be(βp) decay but relies on detection of the ^{10}Be daughter nucleus. This longlived (1.5 10^{6} years) nucleus can be detected via accelerator mass spectrometry (AMS). Our Cu samples will be chemically prepared for the AMS measurements in March 2016 and the ^{10}Be content in each sample measured at the AMS facility VERA soon after. If a background of ^{10}Be were present from directly produced ^{10}Be or from decay of ^{11}Li,

the measured ^{10}Be signal will differ from the ^{11}Be mass dependence. We can therefore conclusively confirm or reject our previous result and will furthermore obtain a new and more accurate value for the branching ratio of the beta-delayed proton decay.

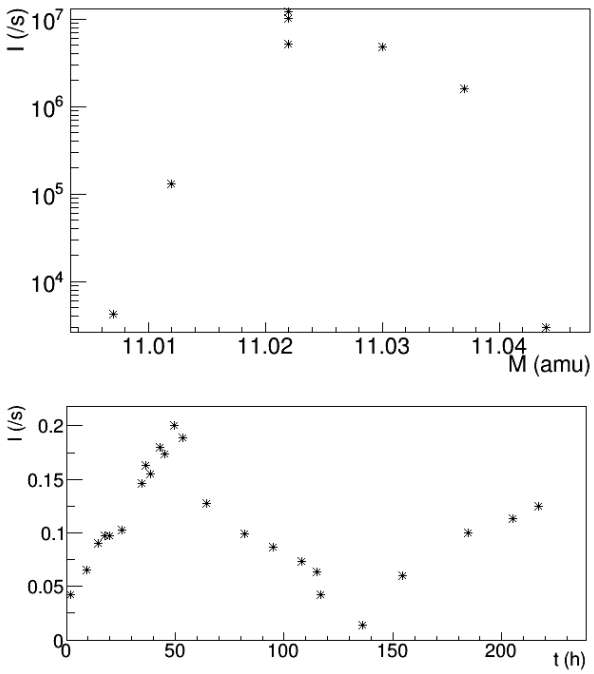

Fig. 1: Top: Mass scan showing the intensity of ^{11}Be as a function of the separator mass setting. Bottom: Recorded ^{24}Na activity as function of time.

Several contamination lines were observed during the experiment and the subsequent calibration phase. Most interesting is the clear identification of ^{24}Na activity (15 h halflife, see figure 1 lower panel). The activity increased during ^{11}Be collection, then decayed after the proton beam was stopped and the valve to our beamline closed, and finally rose again as protons were put unto the GPS target for the following experiment. This final rise shows that the activity was not located in our beamline, but must be situated somewhere else in the ISOLDE hall.

[1] K. Riisager et al., Phys. Lett. B732 (2014) 305
[2] D. Baye and E.M. Tursonov, Phys. Lett. B696 (2011) 464

Beta-delayed neutron spectroscopy with VANDLE at IDS

Results of experiment IS599 and IS600

A. Gottardo and M. Madurga
(for IDS and VANDLE collaborations)

The study of β decay in neutron-rich nuclei has proved to be an effective way to investigate nuclear structure. When going far from stability, the β-decay Q value increases well above 10 MeV in certain regions of the nuclide chart. Furthermore, the neutron separation threshold lowers to a few MeVs in neutron-rich nuclei. As a consequence, β-delayed neutron spectroscopy is required for complete decay measurements. These studies aim to assess the nuclear-structure dependence of the Gamow-Teller strength distribution, which has been thought to be purely statistical [1] until recent times.

VANDLE – IDS setup

The ISOLDE Decay Station supplies a basic framework for decay experiments at the ISOLDE. Radioactive species are implanted in a tape collection system capable of moving away activity in 600 ms. Beta detection and start signal for time of flight was provided by a highly efficient, 90% total, plastic scintillator assembly. Two high purity Germanium clovers, 2% efficiency at 1 MeV, were installed for γ and n-gamma coincidences.

Neutron detection capability was provided by the Versatile Array of Neutron Detectors at Low Energies (VANDLE) [2,3]. VANDLE is a neutron time-of-flight (TOF) detector based on small individual modules. As installed at ISOLDE it consisted of 26 medium-size, 3x6x120 cm^3 at 100 cm, plastic detectors and 12 small-size modules, 3x3x60 cm^3 at 50 cm. The total angular acceptance was 21.8% of 4π. We achieved large sensitivity, 40% detection efficiency at 1 MeV, thanks to the low detection thresholds possible with two PMT configuration and digital electronics [3].

VANDLE Campaign at ISOLDE: IS599 and IS600

The first experiment, IS599, studied the neutron-rich $^{51-53}$Ca via the β decay of $^{51-53}$K. The purpose was to study the position of the $f_{7/2}$ shell in ^{53}Ca and compare it with shell model calculations including three-body forces with different parameters. Moreover, the study of one- and two-neutron emission will also enable to reconstruct the Gamow-Teller strength distribution up to the Q value. This will provide another sensitive probe for nuclear models. Analysis is ongoing. An addendum to this beam time of five days has been approved by the PAC. The goal is to study the decay of ^{54}K to ^{54,53}Ca, to clarify questions about the recently-discovered N=34 subshell closure.

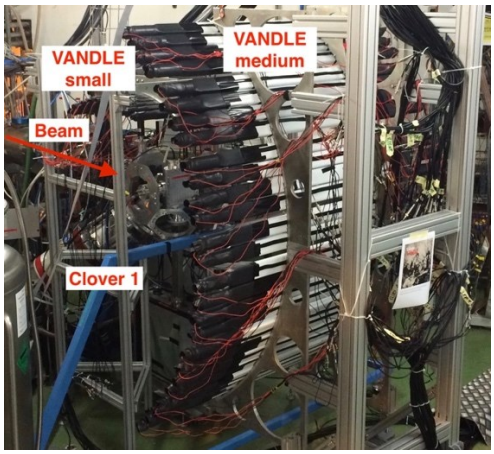

Fig. 1: VANDLE-IDS setup during the IS599-600 campaign. Two germanium clovers along with 26 medium VANDLE bars and 12 small bars were used to obtain 2% gamma and 9% neutron efficiencies.

The second experiment, IS600, studied the β decay of r-process waiting points ^{130,132}Cd. The β-decay half-lives of N=82,84 even isotopes are important parameters to calculate the abundance of the A=130 r-process peak. These in turn are determined by the energy window and the location of the first 1^+ state in the In daughters, whose importance in drawing the majority of the decay strength in ^{130}In was stablished in the measurement by I. Dillmann et al. at ISOLDE [4]. Subsequent measurements stablished a large ^{132}Cd neutron branching ratio, P_n>70%. This suggested the entirety of the Gamow-Teller strength populates neutron unbound states, including the crucial first 1^+ state in ^{83}Go. The neutron time-of-flight spectrum measured with VANDLE shows the majority of the neutron emission occurs from a single state or cluster of states within 100 keV. This clearly points to the presence of a weakly fragmented 1^+ state in ^{132}In. Analysis is currently ongoing.

[1] J.C. Hardy et al, Nucl. Phys A305, 15 (1978)
[2] S.V. Paulauskas et al, Nucl. Inst. And Meth. A737, 22 (2014).
[3] W.A. Peters et al. submitted to Nucl. Inst. And Meth. A.
[4] I. Dillmann et al., Phys. Rev. Lett. 91, 162503 (2003).

Coulomb excitation

Shape coexistence in neutron-rich Strontium isotopes at N=60

Results of experiment IS451

Emmanuel Clément, Magda Zielińska
(for the IS451 collaboration)

Neutron-rich A~100 nuclei are among the best examples of interplay of microscopical and macroscopical effects in nuclear matter. A dramatic onset of quadrupole deformation is observed in the neutron-rich Zr and Sr isotopes at N=60, making this region an active area of experimental and theoretical studies. This rapid shape transition is accompanied by the appearance of low-lying 0^+_2 states that, for N<60, can be interpreted as a deformed configuration that becomes the ground state at N=60, while the spherical ground-state configuration of the isotopes with N<60 becomes non-yrast for those with N≥60.

Low-energy Coulomb excitation experiments were performed in 2007 and 2011 to study properties of coexisting structures in 96,98Sr (N=58,60) using post-accelerated exotic Sr beams from REX-ISOLDE. The experiments were carried out in the particle-gamma coincidence mode using the MINIBALL HPGe array coupled to an annular Double Sided Silicon Detector. Several different targets were used in order to make use of the dependence of the Coulomb excitation cross section on the atomic numbers of collision partners: ^{109}Ag and ^{120}Sn in the case of ^{96}Sr, ^{60}Ni and ^{208}Pb for ^{98}Sr. For ^{96}Sr, the $2^+_1 \rightarrow 0^+_1$ transition was observed together with excitation of target nuclei and a weak transition corresponding to the 0^+_2 deexcitation. For ^{98}Sr, the rotational ground-state band was populated up to spin 8^+, and the decay of the 2^+_2 state was also observed (Fig. 1).

Reduced transition probabilities and spectroscopic quadrupole moments were extracted from the measured differential Coulomb excitation cross sections. The results support the scenario of shape transition at N=60 giving rise to coexistence of two very different configurations in ^{96,98}Sr. In ^{96}Sr, the spectroscopic quadrupole moment of the first 2^+ state was found to be small and negative, corresponding to a weak prolate deformation. In ^{98}Sr, the large and negative spectroscopic quadrupole moments in the ground state band prove its well-deformed prolate character, while the value close to zero obtained for the 2^+_2 state confirms that a spherical configuration coexists with the deformed configuration of the ground state.

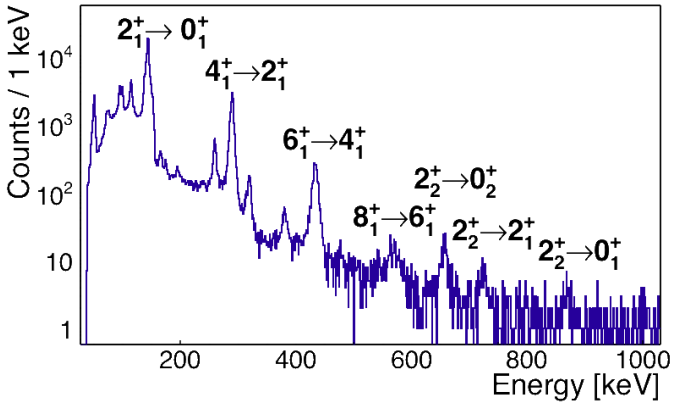

Fig. 1: Gamma-ray spectrum of ^{98}Sr, Coulomb excited on a ^{208}Pb target. The transitions not originating from ^{98}Sr are attributed to the beam contaminant ^{98}Rb.

The comparison of the B(E2) values and the spectroscopic quadrupole moments between the 2^+_1 state in ^{96}Sr and the 2^+_2 state in ^{98}Sr underlines their similarity and further supports the shape inversion when crossing the N=60 line. Furthermore, a very small mixing between the coexisting structures was determined from measured intra-band transition probabilities in ^{98}Sr. This effect has been attributed to the rapidity of the shape change at N=60: a larger mixing would give rise to a more gradual transition from spherical to deformed ground state in Sr isotopes, like what is observed in other areas of shape coexistence, for example neutron-deficient Kr [1] and Hg [2] isotopes.

The results, together with a detailed comparison with new beyond-mean-field calculations, have recently been published [3] and a second publication is in preparation.

[1] E. Clément et al., Phys. Rev. C 75, 054313 (2007).
[2] N. Bree et al., Phys. Rev. Lett. 112, 162701 (2014).
[3] E. Clément, M. Zielińska et al., Phys. Rev. Lett. 116, 022701 (2016)

First Coulomb-excitation studies at 4 MeV/A: ^{74,76}Zn

Results of experiment IS557

Andres Illana, Magda Zielińska
(for the IS557 collaboration)

Shell evolution in the vicinity of the spherical nucleus ^{68}Ni has recently attracted many theoretical and experimental investigations. By now it has been clearly established that the presumed subshell closure at N=40 is not very pronounced. While the intruder character of the $1g_{9/2}$ and $2d_{5/2}$ neutron orbital induces collectivity by pair excitations from the *fp* shell into the $g_{9/2}$ orbital, the parity change hinders quadrupole excitations and therefore mimics the properties of a doubly magic nucleus in ^{68}Ni, i.e., a high 2^+_1 energy and a low B(E2; $2^+ \rightarrow 0^+$) value. Adding valence nucleons to the N=40 open shell leads to a rapid increase of collectivity, with an interplay of both collective and single-particle degrees of freedom. Such rapid changes indicate underlying complex effects and make this region ideal for testing theoretical calculations. While measurements of B(E2; $2^+ \rightarrow 0^+$) values are useful to investigate the evolution of collectivity along isotopic chains, even more insight can be gained by measuring lifetimes of higher-lying states.

Low-energy Coulomb excitation experiment to study properties of states beyond 2^+_1 in ^{74,76}Zn was the first ever to use beams post-accelerated to 4 MeV/A from the HIE-ISOLDE facility. The experiment was performed in October-November 2015, using the MINIBALL HPGe array working in coincidence with an annular CD detector. The intensities of laser ionised ^{74,76}Zn beams at the target position were 10^6 and 5 10^5 pps, respectively. In addition to beams from HIE-ISOLDE, which was operated only during the day, the ^{74,76}Zn beams could be delivered at 2.85 MeV/A outside working hours. Figure 1 presents a comparison of γ-ray spectrum for ^{74}Zn at two beam energies. A clear enhancement of multi-step Coulomb excitation at increased beam energy is observed, demonstrating new experimental opportunities that open thanks to HIE-ISOLDE.

In the ongoing analysis, we are aiming at the determination of the lifetime of the 4^+ state, for which results of earlier measurements [1,2] are contradictory.

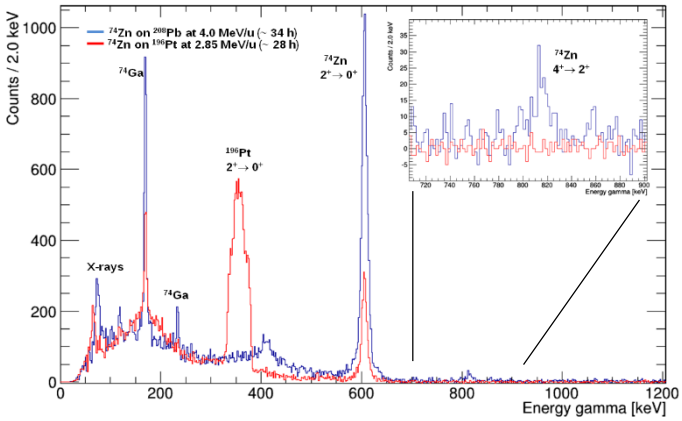

Fig. 1: Gamma-ray spectrum of ^{74}Zn, Coulomb excited at two beam energies: 4 MeV/A beam on ^{208}Pb target (blue line) and 2.85 MeV/A beam on ^{196}Pt target (red line). Only a small part of the data has been taken into account. Population of higher-lying states is clearly enhanced at increased beam energy.

[1] J. Van de Walle *et al.*, Phys. Rev. C 79 (2009) 014309
[2] C. Louchart *et al.*, Phys. Rev. C 87 (2013) 054302

Support and contacts

How to obtain access to the ISOLDE hall

1. Use the online pre-registration tool [1] which should be launched by your team leader or register at the CERN Users office[2] (Opening hours: 08:30 - 12:30 and 14:00 – 16:00 but closed Wednesday mornings). You need to bring
    a. Registration form **signed by your team leader or deputy**[3]
    b. Home Institution Declaration[4] **signed by your institute's administration (HR).**
    c. Passport
2. Get your CERN access card in Building 55

With this registration procedure you become a **CERN user**.

3. Follow the online CERN safety introduction course:

a. If you have a CERN account, you can access the Safety Awareness course on-line at the web page http://sir.cern.ch, from your computer, inside or outside CERN.

b. If you have not activated your CERN account, there are some computers available for use without the need to log in on the first floor of building 55 (Your CERN badge will be needed in order to prove your identity).

4. Complete the following online courses via http://sir.cern.ch:
    a. ISOLDE RP course "ISOLDE - Experimental Hall - Radiation Protection - Fundamentals",
    b. RP course for Supervised Areas " Radiation Protection - Supervised Area",
    c. Electrical Safety - Awareness Course http://sir.cern.ch.
    If you have not activated your CERN account see 3b.
5. Obtain a Permanent radiation dosimeter at the Dosimetry service, located in Building 55[5] (Opening hours: Mon. to Fri. 08:30 – 12:00). If you do not need the dosimeter in the following 2 months it should be returned to the Dosimetry service at the end of your visit.
    The "certificate attesting the suitability to work in CERN's radiation areas" [6] signed by your institute will be required.
6. Follow the 2 hour practical RP safety course and the new 2 hour Electrical Awareness Module for which you will have to register in advance[7]. These take place on **Tuesday afternoons** from 13:00 until 17:00 at the training centre in Prevessin. If you do not have your own transport, you can take CERN shuttle 2 from building 500. The timetable for this is here.
7. Apply for access to "ISOHALL" using EDH: https://edh.cern.ch/Document/ACRQ. This can be done by any member of your collaboration (typically the contact person) having an EDH account[8]. Access to the hall is from the Jura side via your dosimeter.

Find more details about CERN User registration see the Users Office website. For the latest updates on how to access the ISOLDE Hall see the ISOLDE website.

New users are also requested to visit the ISOLDE User Support office while at CERN.

Opening hours:

Monday to Friday 08:30-12:30

[1] For information see http://usersoffice.web.cern.ch/new-registration
[2] http://cern.ch/ph-dep-UsersOffice (Building 61, open 8:30-12:30 and 14:00-16:00, closed Wednesday morning).
[3] Make sure that the registration form is signed by your team leader before coming to CERN or that it can be signed by the team leader or deputy upon arrival.
[4] The Home Institute Declaration should not be signed by the person nominated as your team leader.
[5] http://cern.ch/service-rp-dosimetry (open *only in the mornings* 08:30 - 12:00).
[6] The certificate can be found via http://isolde.web.cern.ch/get-access-isolde-facility
[7] For Information about how to register see http://isolde.web.cern.ch/get-access-isolde-facility
[8] Eventually you can contact Jenny or the Physics coordinator.

Contact information

ISOLDE User Support

Jenny Weterings

Jennifer.Weterings@cern.ch

+41 22 767 5828

Chair of the ISCC

Yorick Blumenfeld

yorick@ipno.in2p3.fr

+33 1 69 15 45 17

Chair of the INTC

Klaus Blaum

Klaus.Blaum@mpi-hd.mpg.de

+49 6221 516 851

ISOLDE Physics Section Leader

Maria J.G. Borge

mgb@cern.ch

+41 22 767 5825

ISOLDE Physics Coordinator

Karl Johnston

Karl.Johnston@cern.ch

+41 22 767 3809

ISOLDE Technical Coordinator

Richard Catherall

Richard.Catherall@cern.ch

+41 22 767 1741

HIE-ISOLDE Project Leader

Yacine Kadi

Yacine.Kadi@cern.ch

+41 22 767 9569

More contact information at

http://isolde.web.cern.ch/contacts/isolde-contacts and at http://isolde.web.cern.ch/contacts/people